PHYSICAL REVIEW D **91,** 054031 (2015)

Charmed-strange mesons revisited: Mass spectra and strong decays

Qin-Tao Song,[1,2,4,*] Dian-Yong Chen,[1,2,†] Xiang Liu,[2,3,‡] and Takayuki Matsuki[5,6,§]

[1]*Nuclear Theory Group, Institute of Modern Physics of CAS, Lanzhou 730000, China*
[2]*Research Center for Hadron and CSR Physics, Lanzhou University and Institute of Modern Physics of CAS, Lanzhou 730000, China*
[3]*School of Physical Science and Technology, Lanzhou University, Lanzhou 730000, China*
[4]*University of Chinese Academy of Sciences, Beijing 100049, China*
[5]*Tokyo Kasei University, 1-18-1 Kaga, Itabashi, Tokyo 173-8602, Japan*
[6]*Theoretical Research Division, Nishina Center, RIKEN, Saitama 351-0198, Japan*

(Received 21 January 2015; published 25 March 2015)

Inspired by the present experimental status of charmed-strange mesons, we perform a systematic study of the charmed-strange meson family in which we calculate the mass spectra of the charmed-strange meson family by taking a screening effect into account in the Godfrey-Isgur model and investigate the corresponding strong decays via the quark pair creation model. These phenomenological analyses of charmed-strange mesons not only shed light on the features of the observed charmed-strange states, but also provide important information on future experimental search for the missing higher radial and orbital excitations in the charmed-strange meson family, which will be a valuable task in LHCb, the forthcoming Belle II, and PANDA.

DOI: 10.1103/PhysRevD.91.054031 PACS numbers: 14.40.Lb, 12.38.Lg, 13.25.Ft

I. INTRODUCTION

As experiments have largely progressed in the past decade, more and more charmed-strange states have been reported [1]. Facing abundant experimental observations, we need to provide an answer, as one crucial task, to the question of whether these states can be identified in the charmed-strange meson family, which is not only a valuable research topic relevant to the underlying structure of the newly observed charmed-strange states, but also helpful in establishing the charmed-strange meson family step by step.

It is a suitable time to give a systematic study of the charmed-strange meson family, which includes two main topics, i.e., the mass spectrum and strong decay behavior. At present, we have abundant experimental information of charmed-strange states which can be combined with the theoretical results to carry out the corresponding phenomenological study.

As the first key step of whole study of the charmed-strange meson family, the investigation of the mass spectrum of charmed-strange mesons should reflect how a charm quark interacts with a strange antiquark. Godfrey and Isgur proposed the so-called Godfrey-Isgur (GI) model to describe the interaction between q and $\bar{q}$ quarks inside of mesons [2] some 30 years ago. Although the GI model has achieved great success in reproducing/predicting the low lying mesons, there exist some difficulties when reproducing the masses of higher radial and orbital excitations, which is because the GI model is a typical quenched model. A typical example of this defect appears in the low mass puzzle of $D_{s0}^{*}(2317)$ [3–6] and $D_{s1}(2460)$ [4–7], where the observed masses of $D_{s0}^{*}(2317)$ and $D_{s1}(2460)$ are far lower than the corresponding results calculated using the GI model. A common feature of higher excitations is that they are near the thresholds of meson pairs, which can interact with these higher excitations with the Okubo-Zweig-Iizuka (OZI)-allowed couplings. Hence, it is unsuitable to use the quenched GI model to describe the mass spectrum of a higher excited meson and, alternatively, we need to adopt an unquenched model. Although there have been a couple of works studying heavy-light systems including charmed-strange mesons together with their decay modes [8–15], we would like to modify the GI model in this work such that the screening effect is introduced to *reflect the unquenched peculiarity.* In the following section, we present a detailed introduction to the modified GI model.

In this work, we revisit the mass spectrum of the charmed-strange meson to apply the modified GI model and compare our results with those of the former GI model and experimental data. We would like to see whether this treatment improves the description of the charmed-strange meson spectrum to make the modified GI model reliable. We try further to obtain information of wave functions of charmed-strange mesons, which is important as an input in calculating the decay behavior of the two-body OZI-allowed decay of charmed-strange mesons.

Together with the study of the mass spectrum of charmed-strange mesons, it is important to know the

*songqint@impcas.ac.cn
†Corresponding author.
chendy@impcas.ac.cn
‡Corresponding author.
xiangliu@lzu.edu.cn
§matsuki@tokyo-kasei.ac.jp

TABLE I. Experimental information of the observed charmed-strange states.

State	Mass (MeV) [1]	Width (MeV) [1]	First observation	Observed decay modes
D_s	1968.49 ± 0.33			
D_s^*	2112.3 ± 0.5	<1.9		
$D_{s0}^*(2317)$	2317.8 ± 0.6	<3.8	*BABAR* [3]	$D_s^+\pi^0$ [3]
$D_{s1}(2460)$	2459.6 ± 0.6	<3.5	CLEO [4]	$D_s^{*+}\pi^0$ [4]
$D_{s1}(2536)$	2535.12 ± 0.13	0.92 ± 0.05	ITEP, SERP [23]	$D_s^{*+}\gamma$ [23]
$D_{s2}^*(2573)$	2571.9 ± 0.8	$16^{+5}_{-4} \pm 3$ [24]	CLEO [24]	D^0K^+ [24]
$D_{sJ}^*(2632)$[a]	$2632.5 \pm 1.7 \pm 5.0$ [25]	< 17 [25]	SELEX [25]	D^0K^+ [25]
$D_{s1}^*(2700)$	$2688 \pm 4 \pm 3$ [26]	$112 \pm 7 \pm 36$ [26]	*BABAR* [26]	DK [26]
	$2708 \pm 9^{+11}_{-10}$ [27]	$108 \pm 23^{+36}_{-31}$ [27]	Belle [27]	D^0K^+ [27]
	$2710 \pm 2^{+12}_{-7}$ [28]	$149 \pm 7^{+39}_{-52}$ [28]	*BABAR* [28]	$D^{(*)}K$ [28]
	$2709.2 \pm 1.9 \pm 4.5$ [29]	$115.8 \pm 7.3 \pm 12.1$ [29]	LHCb [29]	DK [29]
$D_{sJ}^*(2860)$	$2856.6 \pm 1.5 \pm 5.0$ [26]	$47 \pm 7 \pm 10$ [26]	*BABAR* [26]	DK [26]
	$2862 \pm 2^{+5}_{-2}$ [28]	$48 \pm 3 \pm 6$ [28]	*BABAR* [28]	$D^{(*)}K$ [28]
	$2866.1 \pm 1.0 \pm 6.3$ [29]	$69.9 \pm 3.2 \pm 6.6$ [29]	LHCb [29]	DK [29]
$D_{s3}^*(2860)$	$2860.5 \pm 2.6 \pm 2.5 \pm 6.0$ [30,31]	$53 \pm 7 \pm 4 \pm 6$ [30,31]	LHCb [30,31]	$\bar{D}^0K^-$ [30,31]
$D_{s1}^*(2860)$	$2859 \pm 12 \pm 6 \pm 23$ [30,31]	$159 \pm 23 \pm 27 \pm 72$ [30,31]	LHCb [30,31]	$\bar{D}^0K^-$ [30,31]
$D_{sJ}(3040)$	$3044 \pm 8^{+30}_{-5}$ [28]	$239 \pm 35^{+46}_{-42}$ [28]	*BABAR* [28]	D^*K [28]

[a]Since $D_{sJ}^*(2632)$ was only reported by SELEX [25] and not confirmed by other experiments [32], we do not include this state in our review of this work.

properties of charmed-strange mesons when investigating their decay behavior. We will adopt the quark pair creation (QPC) model [16–22] to calculate the two-body OZI-allowed decay of charmed-strange mesons where the corresponding partial and total decay widths are calculated. Through this study, we can further test different possible assignments to the observed charmed-strange states. In addition, we can predict the decay behavior of their partners, which are still missing from experiments. This information is important for experimenters to search further for these missing charmed-strange mesons, which will be a main task of future experiments.

This work is organized as follows. After the Introduction, we will briefly review the research status of the observed charmed-strange states in Sec. II. In Sec. III, the GI model is briefly introduced and we give the detailed illustration of how to modify the GI model by introducing the screening effect. The mass spectrum of charmed-strange mesons together with wave functions is calculated using the modified GI model. Furthermore, the comparison of our results with experimental data and results from the former GI model is given here. With these preparations, in Sec. IV we further study the two-body OZI-allowed strong decay behaviors of charmed-strange mesons through the QPC model and briefly introduce this model. Next, we perform the phenomenological analysis by combining our results with the experimental data. The paper ends with a summary in Sec. V.

II. CONCISE REVIEW OF THE OBSERVED CHARMED-STRANGE STATES

In this section, we briefly review the experimental and theoretical status on charmed-strange mesons. First, in Table I we collect the experimental information of the observed charmed-strange states, which include resonance parameters and the corresponding experiments. Since $D_s^{\pm}$ and $D_s^{*\pm}$ have been established to be $1S$ $c\bar{s}$ mesons, our review mainly focuses on possible candidates of higher radial and orbital excitations in the charmed-strange meson family.

A. $D_{s1}(2536)$ and $D_{s2}^*(2573)$

Prior to 2013, there were only two good candidates for the $1P$ states in the charmed-strange meson family, $D_{s1}(2536)$ and $D_{s2}^*(2573)$.

As a charmed-strange meson with $J^P = 1^+$, $D_{s1}(2536)$ was first observed in 1987 by analyzing the $D_s^*\gamma$ invariant mass spectrum of the $\bar{\nu}N$ scattering process [23], where the measured mass is (2535 ± 28) MeV. Later, the ARGUS Collaboration observed this state in the $D^{*+}K^0$ final state, where its mass and width are $M = (2536 \pm 0.6 \pm 2.0)$ MeV and $\Gamma < 4.6$ MeV [33], respectively. Since there does not exist the $D_{s1}(2536)$ signal in the D^+K^0 invariant mass spectrum, $D_{s1}(2536)$ has an unnatural spin-parity [33]. In 1993, the CLEO Collaboration measured the ratio of $\Gamma(D_{s1}(2536) \to D_s^*\gamma)$ to $\Gamma(D_{s1}(2536) \to D^*K)$, which is [34]

$$\frac{\Gamma(D_{s1}(2536) \to D_s^*\gamma)}{\Gamma(D_{s1}(2536) \to D^*K)} < 0.42. \quad (1)$$

The $D_{s1}(2536)$ has been confirmed by other groups in different channels [35–43]. The *BABAR* Collaboration reported this state in the $D_s^+\pi^+\pi^-$ invariant mass spectrum [6]. The Belle Collaboration observed the $D_{s1}(2536) \to D^+\pi^-K^+$ decay mode [44], where the ratio $\mathcal{B}(D_{s1}^+(2536) \to D^+\pi^-K^+)/\mathcal{B}(D_{s1}^+(2536) \to D^{*+}K^+) = (3.27 \pm 0.18 \pm 0.37)\%$ was obtained. In addition, the measurement of

the angular distribution of the $D_{s1}(2536)^+ \to D^{*+}K_S^0$ indicates that $D_{s1}(2536)^+ \to D^{*+}K_S^0$ dominantly occurs via an S-wave with $\Gamma(D_{s1}(2536)^+ \to D^{*+}K_S^0)_{S\text{-wave}}/\Gamma(D_{s1}(2536)^+ \to D^{*+}K_S^0)_{\text{total}} = (0.72 \pm 0.05 \pm 0.01)$. The mass value and narrow width of $D_{s1}(2536)$ are consistent with the theoretical expectation of the charmed-strange meson as $J^P = 1^+$ [45].

In 1994, the CLEO Collaboration observed a charmed-strange meson $D_{s2}^*(2573)$ in the D^0K^+ invariant mass spectrum [24], where the measured resonance parameters are $M = (2573^{+1.7}_{-1.6} \pm 0.8 \pm 0.5)$ MeV and $\Gamma = (16^{+5}_{-4} \pm 3)$ MeV. In addition, an upper limit of the following ratio was given:

$$\frac{\mathcal{B}(D_{s2}^*(2573)^+ \to D^{*0}K^+)}{\mathcal{B}(D_{s2}^*(2573)^+ \to D^0K^+)} < 0.33, \tag{2}$$

which is from the search for the decay mode $D_{s2}^*(2573)^+ \to D^{*0}K^+$ [24]. At present, $D_{s2}^*(2573)$ is a good candidate of a charmed-strange meson with 1^3P_2 since its mass is consistent with the theoretical prediction [45]. The $D_{s2}^*(2573)$ had subsequently been confirmed by some other collaborations in the D^0K^+ invariant mass spectrum [25,26,38,46,47].

B. $D_{s0}^*(2317)$ and $D_{s1}(2460)$

In 2003, the *BABAR* Collaboration observed a new charmed-strange state near 2.32 MeV in the $D_s^+\pi^0$ invariant mass distribution of the B decay, which is named as $D_{s0}^*(2317)$ [3]. Later, the CLEO Collaboration confirmed this state in the $D_s^+\pi^0$ channel and reported another narrow charmed-strange state $D_{s1}(2460)$ [4]. In addition, the ratio

$$\frac{\mathcal{B}(D_{s0}^*(2317)^+ \to D_s^{*+}\gamma)}{\mathcal{B}(D_{s0}^*(2317)^+ \to D_s^+\pi^0)} < 0.059 \tag{3}$$

was obtained in Ref. [4] while the Belle and *BABAR* collaborations gave the upper bound of this ratio as 0.18 and 0.16, respectively [5,6]. The $D_{s1}(2460)$ was also confirmed by the Belle and *BABAR* collaborations [5–7].

If assigning $D_{s0}^*(2317)$ and $D_{s1}(2460)$ as charmed-strange mesons with quantum numbers $J^P = 0^+$ and $J^P = 1^+$, respectively, there exists the low mass puzzle for $D_{s0}^*(2317)$ and $D_{s1}(2460)$, i.e., the theoretical masses of charmed-strange mesons with 0^+ and 1^+ are 2.48 and 2.53 GeV, respectively, predicted by the old but successful model proposed in Refs. [2,45], whose values are far larger than the corresponding experimental data. These peculiarities have also stimulated theorists' extensive interest in exploring their inner structures and the exotic state explanations to $D_{s0}^*(2317)$ and $D_{s1}(2460)$ were especially proposed in Refs. [48–50].

Since $D_{s0}^*(2317)$ and $D_{s1}(2460)$ are near and below the thresholds of DK and D^*K, respectively, the coupled-channel effect, which is an important nonperturbative QCD effect, should be considered in understanding the low mass puzzle. This means that $D_{s0}^*(2317)$ and $D_{s1}(2460)$ are still categorized as the conventional charmed-strange meson family [51–53].

C. $D_{s1}^*(2700)$

In 2006, the *BABAR* Collaboration observed a broad structure in the DK invariant mass spectrum, which was named as $D_{s1}^*(2700)$ [26] and the mass and width are $M = (2688 \pm 4 \pm 3)$ MeV and $\Gamma = (112 \pm 7 \pm 36)$ MeV, respectively. Later, $D_{s1}^*(2700)$ was confirmed by the Belle Collaboration in the DK invariant mass spectrum of $B \to \bar{D}^0\{D^0K^+\}$ process [27]. The angular momentum and parity of $D_{s1}^*(2700)$ are determined to be $J = 1$ and $P = -$ by the helicity angle distribution and by its decay to two pseudoscalar mesons, respectively. The *BABAR* Collaboration reported the D^*K decay mode of $D_{s1}(2700)$ in Ref. [28] and obtained a ratio of $\mathcal{B}(D_{s1}^*(2710) \to D^*K)$ to $\mathcal{B}(D_{s1}^*(2710) \to DK)$ as [28]

$$\frac{\mathcal{B}(D_{s1}^*(2710) \to D^*K)}{\mathcal{B}(D_{s1}^*(2710) \to DK)} = 0.91 \pm 0.13 \pm 0.12. \tag{4}$$

In 2012, the LHCb Collaboration also observed $D_{s1}^*(2700)$ in the DK mass spectrum [29].

As a vector charmed-strange state, the measured mass of $D_{s1}^*(2700)$ is close to the prediction of the 2^3S_1 charmed-strange meson [2]. The strong decay behavior of a $c\bar{s}$ state of 2^3S_1 is investigated using the QPC model in Ref. [54]. The ratio $\mathcal{B}(D_{s1}^*(2700) \to D^*K)/\mathcal{B}(D_{s1}^*(2700) \to DK)$ evaluated by the effective Lagrangian approach, however, favors the 2^1S_0 assignment for $D_{s1}^*(2700)$ [55]. Besides the decay behavior, the production of $D_{s1}^*(2700)$ from the B meson decay was calculated by a naive factorization method, which shows that $D_{s1}^*(2700)$ could be explained as the first radial excitation of $D_s^*(2112)$ [56].

In Refs. [57,58], $D_{s1}^*(2700)$ was assigned as a mixing of the 2^3S_1 and 1^3D_1 $c\bar{s}$ states, and this assignment can be supported by the study of the decay behavior obtained by the QPC model. The obtained ratio of $\mathcal{B}(D_{s1}^*(2710) \to D^*K)/\mathcal{B}(D_{s1}^*(2710) \to DK)$ is also consistent with the experimental measurement [58] from *BABAR* [28]. In addition, evaluation by the constituent quark model [59] and the Regge phenomenology [60] also supports the assignment of $D_{s1}^*(2710)$ as a mixing of the 2^3S_1 and 1^3D_1 $c\bar{s}$ states. Other than a standard interpretation of $D_{s1}^*(2700)$ as a $c\bar{s}$ state, a molecular state explanation was proposed in Ref. [61], which is based on a potential model.

D. $D_{sJ}^*(2860)$, $D_{s1}^*(2860)$, and $D_{s3}^*(2860)$

The $D_{sJ}^*(2860)$ was first discovered by the *BABAR* Collaboration in the DK invariant mass spectrum of the

inclusive process $e^+e^- \to DKX$ [26]. Its resonance parameters are reported as $M = (2856.6 \pm 1.5 \pm 5.0)$ MeV and $\Gamma = (48 \pm 7 \pm 10)$ MeV. This state was confirmed in the D^*K mode by the *BABAR* Collaboration [28] again and the ratio $\mathcal{B}(D_{sJ}^*(2860)^+ \to D^*K)/\mathcal{B}(D_{sJ}^*(2860)^+ \to DK)$ was measured as

$$\frac{\mathcal{B}(D_{sJ}^*(2860)^+ \to D^*K)}{\mathcal{B}(D_{sJ}^*(2860)^+ \to DK)} = 1.10 \pm 0.15 \pm 0.19. \quad (5)$$

Very recently, the LHCb Collaboration reported their new measurement of the structure around 2.86 GeV in the $\bar{D}^0K^-$ invariant mass distribution of $B_s^0 \to \bar{D}^0K^-\pi^+$ [30,31]. The amplitude analysis of this decay indicates that the structure at $m_{\bar{D}^0K^-} \simeq 2.86$ GeV contains both $J^P = 1^-$ and $J^P = 3^-$ components corresponding to $D_{s1}^*(2860)$ and $D_{s3}^*(2860)$, respectively, where the resonance parameters of $D_{s1}^*(2860)$ and $D_{s3}^*(2860)$ are

$$M_{D_{s1}^*(2860)} = (2859 \pm 12 \pm 6 \pm 23)\ \text{MeV}, \quad (6)$$

$$\Gamma_{D_{s1}^*(2860)} = (159 \pm 23 \pm 27 \pm 72)\ \text{MeV}, \quad (7)$$

$$M_{D_{s3}^*(2860)} = (2860.5 \pm 2.6 \pm 2.5 \pm 6.0)\ \text{MeV}, \quad (8)$$

$$\Gamma_{D_{s3}^*(2860)} = (53 \pm 7 \pm 4 \pm 6)\ \text{MeV}. \quad (9)$$

Before the measurement by the LHCb Collaboration, the properties of $D_{sJ}^*(2860)$ have been widely discussed. The possibility of $D_{sJ}^*(2860)$ as the first radial excitation of $D_{s0}^*(2317)$ has been ruled out due to the observation of $D_{sJ}^*(2860) \to D^*K$ [28]. According to the calculation by the QPC model [54], the Regge phenomenology [60], the chiral quark model [62], and the flux tube model [63], $D_{sJ}^*(2860)$ can be assigned to a 1^3D_3 charmed-strange meson. However, different approaches give different ratios of $\mathcal{B}(D_{sJ}^*(2860) \to D^*K)/\mathcal{B}(D_{sJ}^*(2860) \to DK)$. For example, this ratio was estimated to be 0.36 by the effective Lagrangian method [55] and to be 0.8 by the QPC model [58]. At present calculation, the $J^P = 3^-$ assignment to $D_{sJ}^*(2860)$ is still possible.

In Ref. [58], the $2S$-$1D$ mixing was proposed to explain $D_{sJ}^*(2860)$, where $D_{sJ}^*(2860)$ and $D_{s1}^*(2710)$ are treated as a mixture of the 2^3S_1 and 1^3D_1 states in the charmed-strange meson family. With a proper mixing angle, the ratios of $\mathcal{B}(D_{sJ}^*(2860) \to D^*K)/\mathcal{B}(D_{sJ}^*(2860) \to DK)$ and $\mathcal{B}(D_{sJ}^*(2700) \to D^*K)/\mathcal{B}(D_{sJ}^*(2700) \to DK)$ can be well explained simultaneously. In Ref. [59], the authors proposed a two-state scenario for $D_{sJ}^*(2860)$: one resonance is likely to be the 1^3D_3 state and the other resonance seems to be the higher mixing state of $1^1D_2 - 1^1D_2$. Although the $J^P = 0^+$ assignment to $D_{sJ}^*(2860)$ has been ruled out by the experimental measurement of $D_{sJ}^*(2860) \to D^*K$, the authors of Ref. [64] indicated that there exist two resonances around 2.86 GeV with $J^P = 0^+$ and $J^P = 2^+$. In the DK invariant mass spectrum, the structure near 2.86 GeV should contain these two resonances while, in the D^*K invariant mass spectrum, only one resonance of $J^P = 2^+$ should be included.

Following the measurement by the LHCb Collaboration [30,31], the decay behaviors of $D_{s1}^*(2860)$ and $D_{s3}^*(2860)$ were evaluated by the QPC model [65,66], which show that these states can be good candidates of the $1D$ states in the charmed-strange meson family. By using the QCD sum rule, the masses of the $1D$ charmed-strange mesons were calculated in Ref. [67], which also supports the explanation of the $1D$ charmed-strange mesons. In addition, another study of the decay behaviors of theses states were performed in Ref. [68], where the effective Lagrangian approach was adopted.

Before closing the review of $D_{sJ}^*(2860)$, $D_{s1}^*(2860)$, and $D_{s3}^*(2860)$, we need to comment on the measurement of the ratio in Eq. (5). Since the new measurement by LHCb [30,31] is given, this ratio must be changed according to which state is assigned to D_{sJ}^* in both denomenator and numerator. Thus, we do not suggest adopting the old data of this ratio in Eq. (5) when checking the theoretical result. We also expect a new measurement of this ratio when considering the LHCb results [30,31], which will be helpful to pin down the different explanations.

E. $D_{sJ}(3040)$

Besides confirming $D_{s1}^*(2700)$ and $D_{sJ}^*(2860)$ in the D^*K invariant mass distribution, the *BABAR* Collaboration also observed a new broad structure with mass $M = (3044 \pm 8^{+30}_{-5})$ MeV and width $\Gamma = (239 \pm 35^{+46}_{-42})$ MeV. The negative result of a decay $D_{sJ}(3040) \to DK$ suggests unnatural parity for $D_{sJ}(3040)$.

The observed mass of $D_{sJ}(3040)$ and its unnatural parity are consistent with the quark model prediction for 2^3P_1 charmed-strange meson [2], which is the first radial excitation of $D_{s1}(2460)$. The calculations in the QPC model also support that $D_{sJ}(3040)$ can be categorized as a 1^+ state in a $(0^+, 1^+)$ spin doublet [69] of the heavy quark symmetry. In addition, the calculations in the flux tube model [63], the constitute quark model [59,70], and the effective approach [71] also indicate that the possibility of a $D_{sJ}(3040)$ as a 1^+ charmed-strange meson cannot be ruled out. References [72,73] calculated the decay width of $D_{sJ}(3040)$ as an $n(J^P) = 3(1^+)$ or $n(J^P) = 4(1^+)$ state which is rather large but still compatible with the experimental data. Besides the $J^P = 1^+$ assignment to $D_{sJ}(3040)$, the possibility of $D_{sJ}(3040)$ as a mixture of the 1^3D_2 and 1^1D_2 charmed-strange mesons was discussed with an effective Lagrangian approach [71].

As can be seen in the above review of the status of the observed charmed-strange states, we notice that more and more candidates of higher radial and orbital charmed-strange mesons were reported in the past decade. It is a good opportunity to carry out the systematic study of

charmed-strange mesons now, which will deepen our understanding of the charmed-strange meson family and will provide more abundant information for experimenters to further search for higher radial and orbital charmed-strange mesons in future experiments.

In the following sections, we start to investigate charmed-strange mesons on their mass spectrum and two-body OZI-allowed decay behaviors.

III. MASS SPECTRA

In this work, we employ the modified relativistic quark model to calculate the mass spectra and wave functions of charmed-strange mesons because, owing to the peculiarity of charmed-strange mesons, relativistic effects and unquenched effects cannot be ignored. In 1985, Godfrey and Isgur proposed the GI model to describe the meson spectra with great success, especially for the low lying mesons [2], and Godfrey and Kokoski later studied P-wave heavy-light systems [45]. Since a coupled-channel effect becomes more important for higher radial and orbital excitations, we need to include this effect in calculating the mass spectrum, which motivates us to modify the GI model by introducing the screened potential, which is a partly equivalent description to the coupled-channel effect [74].

In the following, we first give a brief review of the GI model and then present how to introduce the screened potential.

A. Brief review of the Godfrey-Isgur model

The interaction between quark and antiquark in the GI model [2] is described by the Hamiltonian

$$\tilde{H} = (p^2 + m_1^2)^{1/2} + (p^2 + m_2^2)^{1/2} + V_{\rm eff}(\mathbf{p}, \mathbf{r}), \quad (10)$$

where $V_{\rm eff}(\mathbf{p}, \mathbf{r}) = \tilde{H}^{\rm conf} + \tilde{H}^{\rm hyp} + \tilde{H}^{\rm SO}$ is the effective potential of the $q\bar{q}$ interaction. $V_{\rm eff}(\mathbf{p}, \mathbf{r})$ contains two main ingredients. The first one is a short-distance $\gamma^\mu \otimes \gamma_\mu$ interaction of one-gluon exchange and the second is a long-distance $1 \otimes 1$ linear confining interaction which is at first employed by the Cornell group and is suggested by lattice QCD. This effective potential can be obtained by on-shell $q\bar{q}$ scattering amplitudes in the center-of-mass (CM) frame [2].

In the nonrelativistic limit, $V_{\rm eff}(\mathbf{p}, \mathbf{r})$ is transformed into the standard nonrelativistic potential $V_{\rm eff}(r)$:

$$V_{\rm eff}(r) = H^{\rm conf} + H^{\rm hyp} + H^{\rm SO}, \quad (11)$$

with

$$H^{\rm conf} = c + br + \frac{\alpha_s(r)}{r} \boldsymbol{F}_1 \cdot \boldsymbol{F}_2, \quad (12)$$

where $H^{\rm conf}$ is the spin-independent potential and contains a constant term, a linear confining potential, and a one-gluon exchange potential. The subscripts 1 and 2 denote quark and antiquark, respectively. The second term of the rhs of Eq. (11) is the color-hyperfine interaction, i.e.,

$$H^{\rm hyp} = -\frac{\alpha_s(r)}{m_1 m_2}\left[\frac{8\pi}{3}\boldsymbol{S}_1 \cdot \boldsymbol{S}_2 \delta^3(\boldsymbol{r}) + \frac{1}{r^3}\left(\frac{3\boldsymbol{S}_1 \cdot \boldsymbol{r}\boldsymbol{S}_2 \cdot \boldsymbol{r}}{r^2} - \boldsymbol{S}_1 \cdot \boldsymbol{S}_2\right)\right]\boldsymbol{F}_1 \cdot \boldsymbol{F}_2. \quad (13)$$

The third term of the rhs of Eq. (11) is the spin-orbit interaction,

$$H^{\rm SO} = H^{\rm SO(cm)} + H^{\rm SO(tp)}. \quad (14)$$

Here, $H^{\rm SO(cm)}$ is the color-magnetic term and $H^{\rm SO(tp)}$ is the Thomas-precession term, i.e.,

$$H^{\rm SO(cm)} = -\frac{\alpha_s(r)}{r^3}\left(\frac{1}{m_1} + \frac{1}{m_2}\right)\left(\frac{\boldsymbol{S}_1}{m_1} + \frac{\boldsymbol{S}_2}{m_2}\right) \cdot \boldsymbol{L}(\boldsymbol{F}_1 \cdot \boldsymbol{F}_2), \quad (15)$$

$$H^{\rm SO(tp)} = \frac{-1}{2r}\frac{\partial H^{\rm conf}}{\partial r}\left(\frac{\boldsymbol{S}_1}{m_1^2} + \frac{\boldsymbol{S}_2}{m_2^2}\right) \cdot \boldsymbol{L}. \quad (16)$$

In the above expressions, $\boldsymbol{S}_1/\boldsymbol{S}_2$ denotes the spin of the quark/antiquark and $\boldsymbol{L}$ is the orbital momentum between quark and antiquark. $\boldsymbol{F}$ is related to the Gell-Mann matrix by $\boldsymbol{F}_1 = \boldsymbol{\lambda}_1/2$ and $\boldsymbol{F}_2 = -\boldsymbol{\lambda}_2^*/2$. For a meson, $\langle \boldsymbol{F}_1 \cdot \boldsymbol{F}_2 \rangle = -4/3$.

The GI model constructed by Godfrey and Isgur is a relativized quark model, where relativistic effects are embedded into the model in two main ways.

First, a smearing function $\rho_{12}(\boldsymbol{r} - \boldsymbol{r}')$ is introduced to incorporate the effects of internal motion inside a hadron and the nonlocality of interactions between quark and antiquark. A general form is given by

$$\tilde{f}(r) = \int d^3\boldsymbol{r}' \rho_{12}(\boldsymbol{r} - \boldsymbol{r}') f(r'), \quad (17)$$

with

$$\rho_{12}(\boldsymbol{r} - \boldsymbol{r}') = \frac{\sigma_{12}^3}{\pi^{3/2}} \exp\left(-\sigma_{12}^2(\boldsymbol{r} - \boldsymbol{r}')^2\right),$$
$$\sigma_{12}^2 = \sigma_0^2\left[\frac{1}{2} + \frac{1}{2}\left(\frac{4m_1 m_2}{(m_1 + m_2)^2}\right)^4\right] + s^2\left(\frac{2m_1 m_2}{m_1 + m_2}\right)^2, \quad (18)$$

where $\sigma_0 = 1.80$ GeV and $s = 1.55$ are the universal parameters in the GI model and m_1 and m_2 are the masses of the quark and the antiquark, respectively. If $m_1 = m_2$ and both of them become large, σ_{12} also becomes large and

$\rho_{12}(\boldsymbol{r}-\boldsymbol{r}') \to \delta^3(\boldsymbol{r}-\boldsymbol{r}')$, and hence this smearing is effective for a heavy quarkonium because the second term becomes $(sm_1)^2$. If $m_2 \gg m_1$, σ_{12} reaches its minimum and is suitable for describing a heavy-light system like the charmed-strange mesons.

Second, a general formula of the potential should depend on the CM momentum of the interacting quarks. This effect is taken into account by introducing momentum-dependent factors in the interactions and the factors will go to unity in the nonrelativistic limit. In a semiquantitatively relativistic treatment, the smeared Coulomb term $\tilde{G}(r)$ and the smeared hyperfine interactions $\tilde{V}_i$ should be modified according to

$$\tilde{G}(r) \to \left(1+\frac{p^2}{E_1E_2}\right)^{1/2}\tilde{G}(r)\left(1+\frac{p^2}{E_1E_2}\right)^{1/2},$$
$$\frac{\tilde{V}_i(r)}{m_1m_2} \to \left(\frac{m_1m_2}{E_1E_2}\right)^{1/2+\epsilon_i}\frac{\tilde{V}_i(r)}{m_1m_2}\left(\frac{m_1m_2}{E_1E_2}\right)^{1/2+\epsilon_i}, \tag{19}$$

where E_1 and E_2 are the energies of the quark and the antiquark in the meson, ϵ_i's are expected to be small numbers for a different type of hyperfine interactions, i.e., the contract, tensor, vector spin-orbit, and scalar spin-orbit potentials, into which $\tilde{V}_i(r)$ are classified. The particular values of ϵ_i and other parameters are given in Table II of Ref. [2].

Diagonalizing the Hamiltonian given by Eq. (10) on a simple harmonic oscillator (SHO) basis and using a variational method, we get the mass spectrum and wave function of a meson. More details of the GI model can be found in the Appendixes of Ref. [2].

B. Modified GI model with the screening effect

Although the GI model has achieved great success in describing the meson spectrum [2], there still exists a discrepancy between the predictions given by the GI model and recent experimental observations. A typical example is that the masses of the observed $D_{s0}(2317)$ [3–6], $D_{s1}(2460)$ [4–7], and $X(3872)$ [75] deviate from the corresponding values expected by the GI model [2]. Later, theorists realized that these discrepancies are partly caused by coupled-channel effects [51–53,76]. Furthermore, another remedy can be made to adjust the masses by screening the color charges at distances greater than about 1 fm [77], which spontaneously creates light quark-antiquark pairs. The screening effect has been confirmed by unquenched lattice QCD and some holographic models [78–81].

Some progress on the study of the meson mass spectrum was made through considering the screening effect [82,83]. In Ref. [82], the authors adopted the screened potential to compute the charmonium spectrum [74]. Mezzoir *et al.* in [83] carried out the investigation of highly excited light unflavored mesons by flattening the linear potential br above a certain saturation distance r_s. However, the study of a screening effect for a heavy-light meson system is still absent at present, which is why we introduce the screening effect into the GI model in this work.

In order to take into account the screening effect, we need to make a replacement in Eq. (12) [84,85] as

$$br \to V^{\rm scr}(r) = \frac{b(1-e^{-\mu r})}{\mu}, \tag{20}$$

where $V^{\rm scr}(r)$ behaves like a linear potential br at short distances and approaches $\frac{b}{\mu}$ at long distances. Then, we further modify $V^{\rm scr}(r)$ as the way given in Eq. (17),

$$\tilde{V}^{\rm scr}(r) = \int d^3\boldsymbol{r}'\rho_{12}(\boldsymbol{r}-\boldsymbol{r}')\frac{b(1-e^{-\mu r'})}{\mu}. \tag{21}$$

By inserting Eq. (18) into the above expression, the concrete expression for $\tilde{V}^{\rm scr}(r)$ is given by

$$\begin{aligned}\tilde{V}^{\rm scr}(r) &= \frac{b}{\mu r}\left[r + e^{\frac{\mu^2}{4\sigma^2}+\mu r}\frac{\mu+2r\sigma^2}{2\sigma^2}\left(\frac{1}{\sqrt{\pi}}\int_0^{\frac{\mu+2r\sigma^2}{2\sigma}}e^{-x^2}dx-\frac{1}{2}\right)\right.\\ &\left. - e^{\frac{\mu^2}{4\sigma^2}-\mu r}\frac{\mu-2r\sigma^2}{2\sigma^2}\left(\frac{1}{\sqrt{\pi}}\int_0^{\frac{\mu-2r\sigma^2}{2\sigma}}e^{-x^2}dx-\frac{1}{2}\right)\right],\end{aligned} \tag{22}$$

with

$$\begin{aligned}\frac{1}{r}\frac{\partial}{\partial r}\tilde{V}^{\rm scr}(r) = \frac{b}{\mu r^2}\Bigg[&e^{\frac{\mu^2}{4\sigma^2}+\mu r}\frac{\mu^2 r+2r^2\sigma^2\mu-\mu}{2\sigma^2 r}\\ &\times\left(\frac{1}{\sqrt{\pi}}\int_0^{\frac{\mu+2r\sigma^2}{2\sigma}}e^{-x^2}dx-\frac{1}{2}\right)+e^{\frac{\mu^2}{4\sigma^2}-\mu r}\\ &\times\frac{\mu^2 r-2r^2\sigma^2\mu+\mu}{2\sigma^2 r}\\ &\times\left(\frac{1}{\sqrt{\pi}}\int_0^{\frac{\mu-2r\sigma^2}{2\sigma}}e^{-x^2}dx-\frac{1}{2}\right)+\frac{\mu}{\sqrt{\pi}\sigma}e^{-\sigma^2r^2}\Bigg],\end{aligned} \tag{23}$$

where $\tilde{V}(r)$ is given in the footnote on this page and $\sigma = \sigma_{12}$ is given by Eq. (18).

In Fig. 1, we compare the r dependence of our $\tilde{V}^{\rm scr}(r)$, the usual linear potential $V(r)=br$, and $\tilde{V}(r) = \int d^3\boldsymbol{r}'\rho_{12}(\boldsymbol{r}-\boldsymbol{r}')br'$.[1] While behaviors of $\tilde{V}^{\rm scr}(r)$ and $\tilde{V}(r)$ are similar to each other at small distances, there exists a difference between $V(r)=br$ and the smeared

[1]The concrete expression for $\tilde{V}(r)$ is given in Ref. [2] as

$$\tilde{V}(r) = br\left[\frac{e^{-\sigma^2r^2}}{\sqrt{\pi}\sigma r}+\left(1+\frac{1}{2\sigma^2r^2}\right)\frac{2}{\sqrt{\pi}}\int_0^{\sigma r}e^{-x^2}dx\right].$$

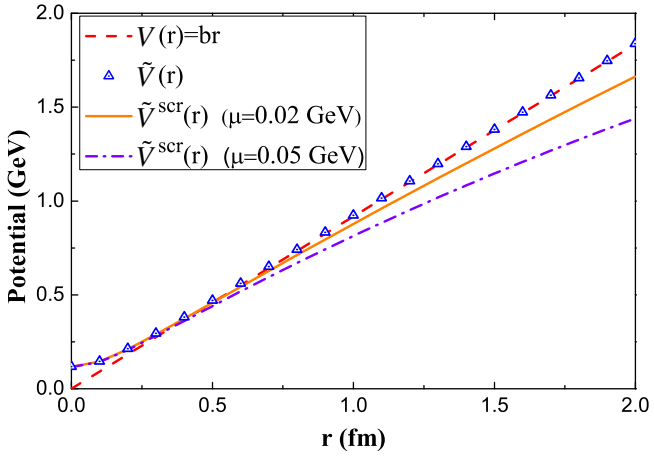

FIG. 1 (color online). The r dependence of $\tilde{V}^{\rm scr}(r)$, $V(r)=br$, and $\tilde{V}(r)=\int d^3\boldsymbol{r}'\rho_{12}(\boldsymbol{r}-\boldsymbol{r}')br'$. Here, we take two values $\mu=0.02$ GeV and $\mu=0.05$ GeV to show $\tilde{V}^{\rm scr}(r)$. Other parameters involved in $\tilde{V}^{\rm scr}(r)$, $V(r)=br$, and $\tilde{V}(r)$ are $m_s=1.628$ GeV, $m_c=0.419$ GeV, $\sigma_0=1.80$ GeV, and $s=1.55$ in the expression of σ_{12}. See Table II in [2].

$\tilde{V}(r)$ reflecting the relativistic effect. There is an obvious difference between $\tilde{V}^{\rm scr}(r)$ and $\tilde{V}(r)$ at large distances due to the screening effect. Comparing a heavy-light system with a heavy quarkonium, the velocity of a light quark in the heavy-light meson is much larger than that of a heavy quark in the quarkonium and, in addition, a radius of the heavy-light meson is also larger than the heavy quarkonium. These facts indicate that we need to consider the relativistic and screening effects when studying the mass spectra of higher radial and orbital excitations of charmed-strange mesons. Furthermore, adjusting μ is to control the power of the screening effect.

C. Numerical results

In the following, we present numerical results of the mass spectrum of the charmed-strange meson family. In Table II, the masses of the charmed-strange mesons are listed using the GI model [2] and our modified GI model, where we take several μ values in $\tilde{V}^{\rm scr}(r)$ to show the μ dependency of our model. Apart from μ, other parameters appearing in our calculation are taken from Ref. [2], with which we can, of course, reproduce the masses obtained in Refs. [2,86]. In Table II, we also give the $R=1/\beta$ values corresponding to charmed-strange mesons, where the R value can be obtained by the relation

$$\int \Psi^{\rm SHO}_{nLM}(\mathbf{p})^2 p^2 d^3\mathbf{p} = \int \Phi(\mathbf{p})^2 p^2 d^3\mathbf{p}. \tag{24}$$

The rhs of Eq. (24) is the root-mean-square momentum, which can be directly calculated through the GI model or the modified GI model. The lhs of Eq. (24) is a definition of the root-mean-square momentum when adopting the SHO wave function. Here, in the momentum space, the SHO wave fuA1161nction is expressed as

$$\Psi^{\rm SHO}_{nLM_L}(\boldsymbol{p}) = R^{\rm SHO}_{nL}(p) Y_{LM_L}(\Omega_p), \tag{25}$$

with the radial wave function

TABLE II. Mass spectrum of the charmed-strange meson family obtained by our modified GI model and the comparison with those calculated by the GI model. Here, we take $\mu=0.01, 0.02, 0.03$, and 0.04 GeV to show the results with the modified GI model. The values in brackets are the obtained $R=1/\beta$ and n denotes the radial quantum number. We emphasize that we do not consider the mixing among states with the same quantum number when presenting the results in this table. μ is in units of GeV, while R is in units of GeV^{-1}.

	GI model [2,86]		Modified GI model							
			$n=1$				$n=2$			
	$n=1$	$n=2$	$\mu=0.01$	$\mu=0.02$	$\mu=0.03$	$\mu=0.04$	$\mu=0.01$	$\mu=0.02$	$\mu=0.03$	$\mu=0.04$
n^1S_0	1979(1.41)	2673(2.00)	1971	1967(1.41)	1963	1960	2661	2646(2.08)	2632	2618
n^3S_1	2129(1.69)	2732(2.08)	2120	2115(1.71)	2111	2106	2719	2704(2.17)	2688	2673
n^1P_1	2550(1.92)	3024(2.17)	2541	2531(1.96)	2522	2512	3001	2979(2.27)	2957	2935
n^3P_0	2484(1.75)	3005(2.13)	2473	2463(1.79)	2454	2444	2982	2960(2.22)	2937	2914
n^3P_1	2552(1.89)	3033(2.22)	2542	2532(1.96)	2522	2512	3010	2988(2.27)	2965	2942
n^3P_2	2592(2.08)	3048(2.27)	2581	2571(2.17)	2561	2551	3026	3004(2.38)	2981	2959
n^1D_2	2910(2.22)	3307(2.38)	2893	2877(2.27)	2861	2844	3277	3247(2.50)	3216	3186
n^3D_1	2899(2.08)	3306(2.27)	2882	2865(2.13)	2848	2831	3275	3244(2.44)	3213	3182
n^3D_2	2916(2.17)	3313(2.38)	2899	2882(2.27)	2865	2848	3283	3252(2.50)	3221	3190
n^3D_3	2917(2.33)	3311(2.44)	2900	2883(2.38)	2867	2850	3281	3251(2.56)	3221	3190
n^1F_3	3199(2.38)	⋯	3175	3151(2.50)	3127	3102	⋯	⋯	⋯	⋯
n^3F_2	3208(2.27)	⋯	3183	3159(2.38)	3134	3109	⋯	⋯	⋯	⋯
n^3F_3	3205(2.33)	⋯	3181	3157(2.44)	3132	3107	⋯	⋯	⋯	⋯
n^3F_4	3190(2.44)	⋯	3167	3143(2.56)	3120	3096	⋯	⋯	⋯	⋯

TABLE III. Comparison of the experimental data and theoretical results. Here, we also list the χ^2 values for different models. The notation L_L is introduced to express mixing states of either ^1L_L or ^3L_L.

	$n^{2S+1}L_J$	Experimental values [1]	GI model [2,86]	Modified GI model[a]
D_s	1^1S_0	1968.49 ± 0.33	1979	1967
D_s^*	1^3S_1	2112.3 ± 0.5	2129	2115
$D_{s1}(2536)$	$1P_1$	2535.12 ± 0.13	2556	2534
$D_{s2}^*(2573)$	1^3P_2	2571.9 ± 0.8	2592	2571
$D_{s1}^*(2700)$	2^3S_1	2709 ± 4	2732	2704
$D_{s1}^*(2860)$	1^3D_1	$2859 \pm 12 \pm 6 \pm 23$ [30,31]	2899	2865
$D_{s3}^*(2860)$	1^3D_3	$2860.5 \pm 2.6 \pm 2.5 \pm 6.0$ [30,31]	2917	2883
$D_{sJ}(3040)$	$2P_1$	$3044 \pm 8^{+30}_{-5}$ [28]	3038	2992
χ^2	...	...	7165	36

[a]The results listed in the last column are calculated via the modified GI model with $\mu = 0.02$ GeV.

$$R_{nL}^{\rm SHO}(p) = \frac{(-1)^n(-i)^L}{\beta^{3/2}}\sqrt{\frac{2n!}{\Gamma(n+L+3/2)}}\left(\frac{p}{\beta}\right)^L e^{-\frac{p^2}{2\beta^2}} \times L_n^{L+1/2}(p^2/\beta^2), \tag{26}$$

where $L_n^{L+1/2}(p^2/\beta^2)$ is an associated Laguerre polynomial with the oscillator parameter β. In the configuration space the SHO wave function is given by

$$\Psi_{nLM_L}^{\rm SHO}(\boldsymbol{r}) = R_{nL}^{\rm SHO}(r)Y_{LM_L}(\Omega_r), \tag{27}$$

where the radial wave function is defined as

$$R_{nL}^{\rm SHO}(r) = \beta^{3/2}\sqrt{\frac{2n!}{\Gamma(n+L+3/2)}}(\beta r)^L e^{\frac{-\beta^2 r^2}{2\beta^2}} L_n^{L+1/2}(\beta^2 r^2). \tag{28}$$

The β is the parameter appearing in the SHO radial wave function given in Eq. (26), which is determined by the above procedure.

In Table III, we further compare the calculated results with the experimental data. Illustrating further a suitable μ value introduced in the modified GI model, we also list the χ^2 values for the GI model and the modified GI model, where χ^2 is defined as

$$\chi^2 = \sum_i \left(\frac{\mathcal{A}_{\rm Th}(i) - \mathcal{A}_{\rm Exp}(i)}{\rm Error}(i)\right)^2, \tag{29}$$

where $\mathcal{A}_{\rm Th}(i)$ and $\mathcal{A}_{\rm Exp}(i)$ are theoretical and experimental values. Error(i) is the experimental error listed in Table III. In Table III, the values of χ^2 are calculated without the contributions from $D_{s0}(2317)$ and $D_{s1}(2460)$. Comparing the χ^2 values for different cases, we find that the modified GI model can well describe the experiments when $\mu = 0.02$ GeV and that the description of the observed charmed-strange spectrum can be obviously improved by the modified GI model with the screening effect. One can clearly see the trend of decreasing masses with increasing μ from Table III.

In Fig. 2, we further list the results obtained by the modified GI model ($\mu = 0.02$ GeV) and make a comparison with the GI model and experimental data. As for D_s, D_s^*, $D_{s1}(2536)$, $D_{s2}^*(2573)$, $D_{s1}^*(2700)$, and the newly observed $D_{s1}^*(2860)$, the mass differences between the experimental data and our theoretical results are less than 10 MeV. While the theoretical mass of $D_{sJ}^*(2860)$ is about 20 MeV lower than the experimental value, we notice that the experimental masses of $D_{s0}^*(2317)$ and $D_{s1}(2460)$ cannot be reproduced by the modified GI model. This discrepancy is caused by the near-threshold effect, which is ignored in the screening effect [74]. In general, the comparison of ten samples of experimental data with our calculated results indicates that the modified GI model is more suitable to describe the experimental data, especially to higher charmed-strange mesons.

We should emphasize that the $n^1P_1 - n^3P_1$ and $n^1D_2 - n^3D_2$ mixtures with $n = 1, 2$ are included in the corresponding calculations listed in Table III and Fig. 2, which is different from the situation in Table II since we need to compare theoretical results with the experimental data.

IV. TWO-BODY OZI-ALLOWED STRONG DECAYS

In addition to the mass spectrum, the decay properties are also crucial features of mesons. The QPC model is successful to calculate OZI-allowed strong decays of mesons. Here, we first give a brief introduction to the QPC model.

A. Brief introduction to the QPC model

The QPC model was proposed by Micu [16] and developed by the Orsay group [17–22]. It assumes that meson decay occurs through a flavor-singlet and color-singlet quark-antiquark pair created from the vacuum. The transition operator T can be expressed as

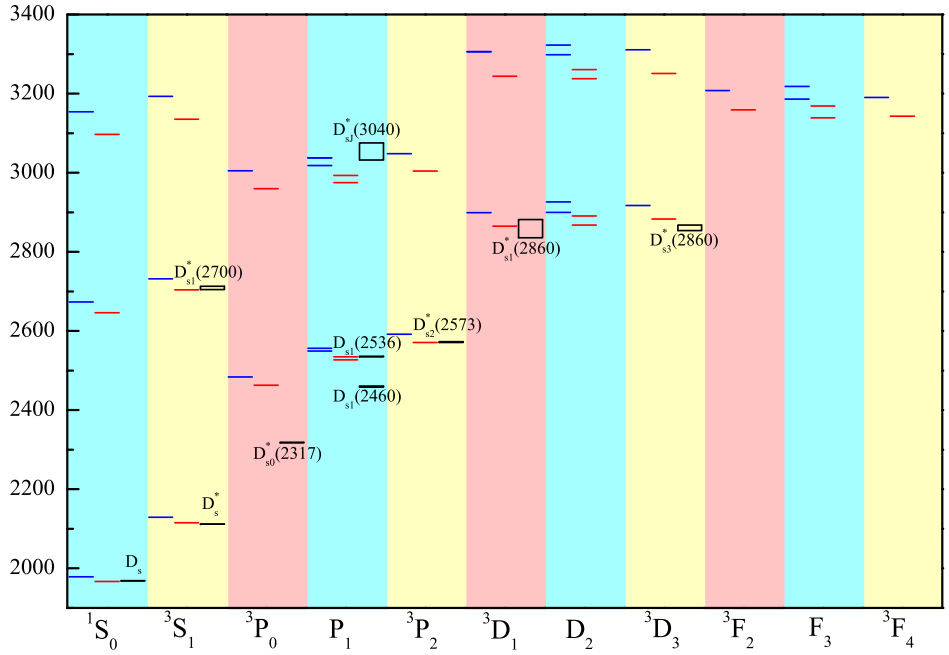

FIG. 2 (color online). Mass spectrum of charmed-strange mesons (in units of MeV). Here, the blue lines stand for the results obtained by the GI model [2,86], while the red lines show the modified GI model with $\mu = 0.02$ GeV. The black rectangles denote the experimental data taken from PDG [1]. The corresponding $^{2S+1}L_J$ quantum numbers are listed in the abscissa. In addition, when there exists a mixture of n^1L_L and n^3L_L states, we use another notation L_L.

$$T = -3\gamma\sum_m \langle 1m;1-m|00\rangle \int d\mathbf{p}_3 d\mathbf{p}_4 \delta^3(\mathbf{p}_3+\mathbf{p}_4) \times \mathcal{Y}_{1m}\left(\frac{\mathbf{p}_3-\mathbf{p}_4}{2}\right)\chi^{34}_{1,-m}\phi^{34}_0(\omega^{34}_0)_{ij}b^\dagger_{3i}(\mathbf{p}_3)d^\dagger_{4j}(\mathbf{p}_4), \tag{30}$$

where $\mathbf{p}_3$ and $\mathbf{p}_4$ denote the momenta of quark and antiquark created from the vacuum, respectively. γ is the parameter which describes the strength of the creation of the quark-antiquark pair. By comparing the experimental widths with theoretical ones of 16 famous decay channels, $\gamma = 8.7$ is obtained for the $u\bar{u}/d\bar{d}$ pair creation [87]. For the $s\bar{s}$ pair creation, we take $\gamma = 8.7/\sqrt{3}$ [17]. $\phi^{34}_0 = (u\bar{u}+d\bar{d}+s\bar{s})/\sqrt{3}$ is the flavor function, while $(\omega^{34}_0)_{ij} = \delta_{ij}/\sqrt{3}$ is the color function, where i and j are the color indices. $\mathcal{Y}_{\ell m}(\mathbf{p}) = |\mathbf{p}|^\ell Y_{\ell m}(\mathbf{p})$ denotes the solid harmonic polynomial. Thus, $\mathcal{Y}_{1m}(\frac{\mathbf{p}_3-\mathbf{p}_4}{2})$ indicates that the angular momentum of the quark-antiquark pair is $L = 1$. The $\chi^{34}_{1,-m}$ means that the total spin angular momentum of the quark-antiquark pair is $S = 1$. Finally, the quantum number of the quark-antiquark pair is contained as $J^{PC} = 0^{++}$ through the coupling of the angular momentum with the spin angular momentum.

The transition matrix of meson A decaying into mesons B and C in the A rest frame is defined as

$$\langle BC|T|A\rangle = \delta^3(\mathbf{p}_B+\mathbf{p}_C)\mathcal{M}^{M_{JA}M_{JB}M_{JC}}, \tag{31}$$

$\mathbf{p}_B$ and $\mathbf{p}_C$ are the momenta of mesons B and C, respectively. $|A\rangle$, $|B\rangle$, and $|C\rangle$ denote the mock states [88]. Taking a meson A as an example, we illustrate the definition of a mock state, i.e.,

$$\begin{aligned}|A(n^{2S+1}L_{JM_J})(\mathbf{p}_A)\rangle &= \sqrt{2E}\sum_{M_S,M_L}\langle LM_L;SM_S|JM_J\rangle\chi^A_{S,M_s} \\ &\times \phi^A\omega^A\int d\mathbf{p}_1 d\mathbf{p}_2\delta^3(\mathbf{p}_A-\mathbf{p}_1-\mathbf{p}_2) \\ &\times \Psi^A_{nLM_L}(\mathbf{p}_1,\mathbf{p}_2)|q_1(\mathbf{p}_1)\bar{q}_2(\mathbf{p}_2)\rangle,\end{aligned} \tag{32}$$

where χ^A_{S,M_s}, ϕ^A, and ω^A are the spin, flavor, and color wave functions, respectively. $\Psi^A_{nLM_L}(\mathbf{p}_1,\mathbf{p}_2)$ is the spacial wave function of a meson A in the momentum space, which can be obtained by the modified GI model. The calculated amplitude $M^{M_{JA}M_{JB}M_{JC}}$ can be converted into the partial wave amplitude M^{JL} via the Jacob-Wick formula [89], i.e.,

$$\mathcal{M}^{JL}(A\to BC) = \frac{\sqrt{2L+1}}{2J_A+1}\sum_{M_{JB},M_{JC}}\langle L0;JM_{JA}|J_AM_{JA}\rangle \times \langle J_BM_{JB};J_CM_{JC}|JM_{JA}\rangle\mathcal{M}^{M_{JA}M_{JB}M_{JC}}. \tag{33}$$

Finally, the decay width can be expressed as

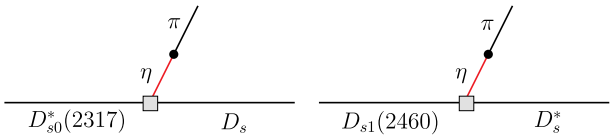

FIG. 3 (color online). The $D^*_{s0}(2317) \to D_s\pi^0$ (left panel) and $D_{s1}(2460) \to D^*_s\pi^0$ (right panel) decays through the $\eta - \pi^0$ mixing.

$$\Gamma = \pi^2 \frac{|\mathbf{p}_B|}{m_A^2} \sum_{J,L} |\mathcal{M}^{JL}|^2. \tag{34}$$

We would like to emphasize the improvement of the present work compared with the former works in Refs. [54,65,69]. In Refs. [54,65,69], authors adopted the SHO wave function to describe a spacial wave function of charmed and charmed-strange mesons, where the β value in the SHO wave function is determined by Eq. (24). This treatment is an approximation for simplifying the calculation since the SHO wave function $\Psi^{\rm SHO}_{nLM_L}(\boldsymbol{p})$ is slightly different from the wave function $\Phi(\boldsymbol{p})$ in Eq. (24). In this work, for the charmed-strange meson A involved in our calculation, we use the numerical wave function directly obtained as an eigenfunction of the modified GI model, which can avoid the uncertainty from the treatment in Eq. (24). For the mesons B and C in the discussed process, we still adopt the SHO wave function, where the corresponding β was calculated in Ref. [45].

In the following concrete calculation, the mass is taken from PDG [1] if there exists the corresponding experimental observation of a charmed-strange meson. If the discussed charmed-strange meson is still missing, we adopt the theoretical prediction from the modified GI model (the results listed in Fig. 2) as the input.

B. Phenomenological analysis of strong decay

In this subsection, we carry out the phenomenological analysis of the strong decays of charmed-strange mesons by combining our theoretical results with the corresponding experimental data.

1. 1P states

If $D^*_{s0}(2317)$ and $D_{s1}(2460)$ are the $1P$ states in the charmed-strange meson family, the OZI-allowed strong decays are forbidden since their masses are below the DK/D^*K thresholds. However, $D^*_{s0}(2317) \to D_s\pi^0$ and $D_{s1}(2460) \to D^*_s\pi^0$ can occur via the $\eta - \pi$ mixing, which is shown in Fig. 3 [90].

For calculating these decays, we need the Lagrangian including the $\eta - \pi^0$ mixing, which can be expressed as [91]

$$\mathcal{L}_{\eta-\pi^0} = \frac{m_\pi^2 f^2}{4(m_u + m_d)} \mathrm{Tr}(\xi m_q \xi + \xi^\dagger m_q \xi^\dagger), \tag{35}$$

where m_q is a light quark mass matrix, $\xi = \exp(i\tilde{\pi}/\mathrm{f}_\pi)$, and $\tilde{\pi}$ is a light meson octet.

Taking $D^*_{s0}(2317) \to D_s\pi^0$ as an example, we illustrate the concrete calculation. The decay amplitude of $D^*_{s0}(2317) \to D_s\pi^0$ reads as

$$\mathcal{M}^{JL}(D^*_{s0}(2317) \to D_s\pi^0) = \mathcal{M}^{JL}(D^*_{s0}(2317) \to D_s\eta) \times \frac{i\sqrt{3}}{4}\delta_{\pi^0\eta}, \tag{36}$$

where the decay amplitude $\mathcal{M}^{JL}(D^*_{s0}(2317) \to D_s\eta)$ can be calculated by the QPC model. The isospin-violating factor $\delta_{\pi^0\eta}$ is due to the $\eta - \pi$ mixing, i.e., [92]

$$\delta_{\pi^0\eta} = \frac{m_d - m_u}{m_s - (m_u + m_d)/2} = \frac{1}{43.7}. \tag{37}$$

Adopting a similar treatment, we can derive the formula of $D_{s1}(2460) \to D^*_s\pi^0$. Here, $D_{s1}(2460)$ with $J^P = 1^+$ is the mixture between the 1^1P_1 and 1^3P_1 states, which satisfies the relation

$$\begin{pmatrix} |D_{s1}(2460)\rangle \\ |D_{s1}(2536)\rangle \end{pmatrix} = \begin{pmatrix} \cos\theta_{1P} & \sin\theta_{1P} \\ -\sin\theta_{1P} & \cos\theta_{1P} \end{pmatrix} \begin{pmatrix} |1^1P_1\rangle \\ |1^3P_1\rangle \end{pmatrix}, \tag{38}$$

where the mixing angle $\theta_{1P} = -54.7°$ is obtained in the heavy quark limit [45,93,94].

The obtained partial widths of $D^*_{s0}(2317) \to D_s\pi^0$ and $D_{s1}(2460) \to D^*_s\pi^0$ are listed in Table IV. We also compare our results with other theoretical predictions from different groups [10,14,49,90,95–99]. In particular, we notice that our results are consistent with the corresponding values given in Ref. [96]. The equality of these two decay widths predicted in Ref. [14] in the heavy quark limit is well satisfied in our case, too.

TABLE IV. Partial widths of $D^*_{s0}(2317) \to D_s\pi^0$ and $D_{s1}(2460) \to D^*_s\pi^0$ (in the unit of keV). Here, we list the width of $D_{s1}(2460) \to D^*_s\pi^0$ with a mixing angle $\theta_{1P} = -54.7° = -\arcsin(\sqrt{2/3})$ in the heavy quark limit.

	This work	Ref. [90]	Ref. [10]	Ref. [95]	Ref. [96]	Ref. [97]	Ref. [98]	Ref. [49]	Ref. [99]	Ref. [14]
$\Gamma(D^*_{s0}(2317) \to D_s\pi)$	11.7	32	21.5	16	∼10	34–44	≃6	10–100	155 ± 70	3.8
$\Gamma(D_{s1}(2460) \to D^*_s\pi)$	11.9	35	21.5	32	∼10	35–51	≃6	⋯	155 ± 70	3.9

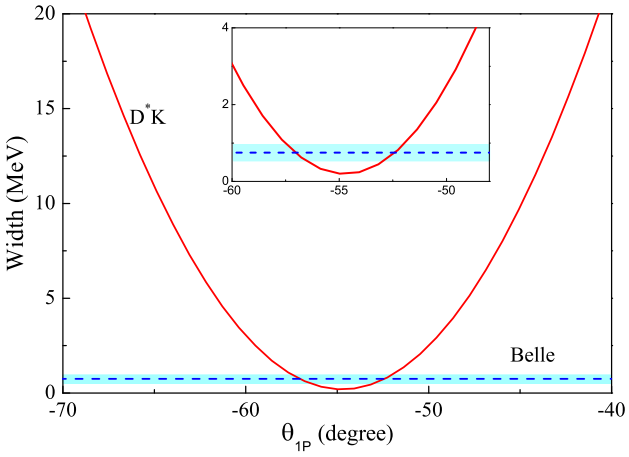

FIG. 4 (color online). The mixing angle θ_{1P} dependence of a decay width $D_{s1}(2536) \to D^*K$.

$D_{s1}(2536)$ with $J^P = 1^+$ is the orthogonal partner of $D_{s1}(2460)$, as shown in Eq. (38). The D^*K channel is its only OZI-allowed decay mode. In Fig. 4, we present the dependence of the partial decay width of $D_{s1}(2536) \to D^*K$ on θ_{1P}, which covers the typical value $\theta_{1P} = -54.7°$ given in the heavy quark limit [45,93,94]. We notice that our result is consistent with the experimental data $\Gamma = 0.92 \pm 0.05$ MeV [42] and $\Gamma = 0.75 \pm 0.23$ MeV [43], when the mixing angle is around $\theta_{1p} = -52.3°$ and $\theta_{1p} = -53.1°$, respectively, which are close to $\theta_{1p} = -54.7°$ of the heavy quark limit. In the heavy quark limit, the decay of $D_{s1}(2536)$ into D^*K can occur only via a D wave because of the conservation of a light degree of freedom, and hence the decay width is expected to be small, as shown in Fig. 4. That is because the experimental mixing angle is very close to the one of the heavy quark limit; it is a model independent result that $D_{s1}(2536)$ and D^*K almost exactly decouple with each other, which has been discussed in Refs. [45,100].

As a good candidate of the charmed-strange meson with 1^3P_2, $D_{s2}(2573)$ decays into DK, D^*K, and $D_s\eta$, with the partial decay widths 5.42, 0.57, and 0.04 MeV, respectively. The total decay width of $D_{s2}(2573)$ can reach up to 6.03 MeV, which is comparable with the experimental values $16^{+5}_{-4} \pm 3$ [24], $10.4 \pm 8.3 \pm 3.0$ [47], and $12.1 \pm 4.5 \pm 1.6$ MeV [46] given by the ARGUS Collaboration and the LHCb Collaboration, respectively. In addition, the branching ratio

$$\frac{\mathcal{B}(D_{s2}(2573) \to D^{*0}K^+)}{\mathcal{B}(D_{s2}(2573) \to D^0K^+)} < 0.33 \tag{39}$$

is also measured by the CLEO Collaboration [24]. In this work, we obtain $\mathcal{B}(D^{*0}K^+)/\mathcal{B}(D^0K^+) = 0.106$, consistent with the present experimental measurement [24]. This value is also close to the one, 0.076, predicted in Ref. [14].

2. 2S and 1D states

Since there is no candidate for the 2^1S_0 charmed-strange meson observed in the experiment, we adopt the theoretical value calculated by the modified GI model as an input, i.e., 2646 MeV. As shown in Table V, $D_s(2^1S_0)$ only decays

TABLE V. Calculated partial decay widths of the OZI-allowed strong decays of the $2S$, $1D$, $3S$, and $2P$ charmed-strange mesons. Units are in MeV. Here, forbidden decay channels are marked by ⋯ and channels marked by □ are the OZI-allowed modes, which are discussed in consideration of the mixing angle dependence.

Channels	D_s (2^1S_0)	D^*_{s1} (2700)	D^*_{s1} (2860)	$D_s(1D(2^-))$ $D_s(1D'(2^-))$	D^*_{s3} (2860)	D_s (2^3P_0)	D_s $(2P(1^+))$	D_s $(2P'(1^+))$	D_s (2^3P_2)	D_s (3^1S_0)	D_s (3^3S_1)
DK	⋯	□	□	⋯	7.46	60.86	⋯	⋯	2.99×10^{-4}	⋯	23.30
D^*K	76.06	□	□	□	5.98	⋯	62.43	20.72	5.30	38.11	36.54
$D_s\eta$	⋯	□	□	⋯	0.15	2.07	⋯	⋯	0.02	⋯	2.19
$D_s\eta'$	⋯	⋯	⋯	⋯	⋯	0.08	⋯	⋯	0.001	⋯	0.40
$D^*_s\eta$	⋯	□	□	□	0.06	⋯	1.61	1.02	0.18	2.56	2.72
$D^*_s\eta'$	⋯	⋯	⋯	⋯	⋯	⋯	⋯	⋯	⋯	⋯	0.07
DK^*	⋯	⋯	□	□	0.37	⋯	39.32	6.50	13.46	3.33	14.92
D^*K^*	⋯	⋯	⋯	⋯	⋯	63.66	48.97	39.60	48.32	18.54	3.30×10^{-5}
$D_s\phi$	⋯	⋯	⋯	⋯	⋯	⋯	1.45	8.05	0.003	0.03	0.07
$D^*_s\phi$	⋯	⋯	⋯	⋯	⋯	⋯	⋯	⋯	⋯	⋯	9.97×10^{-4}
$D^*_0(2400)K$	⋯	⋯	⋯	□	⋯	⋯	14.42	31.13	⋯	38.14	⋯
$D^*_{s0}(2317)\eta$	⋯	⋯	⋯	□	⋯	⋯	1.06	2.41	⋯	5.38	⋯
$D_1(2430)K$	⋯	⋯	⋯	⋯	⋯	3.32	14.31	8.11	14.31	⋯	17.02
$D_1(2420)K$	⋯	⋯	⋯	⋯	⋯	36.16	19.43	10.43	0.75	⋯	5.50
$D_{s1}(2460)\eta$	⋯	⋯	⋯	⋯	⋯	⋯	0.25	0.16	⋯	⋯	3.43
$D_{s1}(2536)\eta$	⋯	⋯	⋯	⋯	⋯	⋯	⋯	⋯	⋯	⋯	0.02
$D^*_2(2460)K$	⋯	⋯	⋯	⋯	⋯	⋯	82.85	3.15	3.90	5.89	9.16
$D^*_{s2}(2573)\eta$	⋯	⋯	⋯	⋯	⋯	⋯	⋯	⋯	⋯	⋯	0.002
Total	76.06	⋯	⋯	⋯	14.02	166.15	285.83	131.28	86.25	111.98	115.35

into D^*K, where the decay width of $D_s(2^1S_0) \to D^*K$ is 76.06 MeV.

In the following, we shall discuss the two observed, $D^*_{s1}(2700)$ and $D^*_{s1}(2860)$, to be an admixture of $D_s(2^3S_1)$ and $D_s(1^3D_1)$ which satisfies the relation

$$\begin{pmatrix} |D^*_{s1}(2700)\rangle \\ |D^*_{s1}(2860)\rangle \end{pmatrix} = \begin{pmatrix} \cos\theta_{SD} & \sin\theta_{SD} \\ -\sin\theta_{SD} & \cos\theta_{SD} \end{pmatrix} \begin{pmatrix} |2^3S_1\rangle \\ |1^3D_1\rangle \end{pmatrix}, \tag{40}$$

where θ_{SD} denotes a mixing angle describing an admixture of $D_s(2^3S_1)$ and $D_s(1^3D_1)$.

The θ_{SD} dependence of the total and partial decay widths of $D^*_{s1}(2700)$ is shown in the Fig. 5. Its main decay modes are DK and D^*K, both of which were observed in the experiments. To compare our results with the experimental data, we take *BABAR*'s measurement in Ref. [28] since the width $\Gamma = (149 \pm 7^{+39}_{-52})$ MeV together with the ratio listed in Eq. (4) was given [28]. As shown in Fig. 5, there exists the common θ_{SD} range, 6.8°–11.2°, in which both the calculated width and the ratio of $D^*_{s1}(2700)$ [28] can overlap with the experimental data. This small θ_{SD} value is consistent with the estimate of θ_{SD} in Ref. [2].

As for the $D^*_{s1}(2860)$ with $J^P = 1^-$ recently observed by the LHCb Collaboration [30,31], which is considered to be a partner of $D^*_{s1}(2700)$, the θ_{SD} dependence of the decay behavior is depicted in Fig. 6. If taking 6.8°–11.2° for the range of θ_{SD} obtained in the study of $D^*_{s1}(2700)$, we find that the obtained total decay width of $D^*_{s1}(2860)$ can reach up to ∼300 MeV, which is comparable with the LHCb data [30,31] and the ratio is $\mathcal{B}(D^*_{s1}(2860) \to D^*K)/\mathcal{B}(D^*_{s1}(2860) \to DK) = 0.6 \sim 0.8$, which can be tested in future experiments. Our study also shows

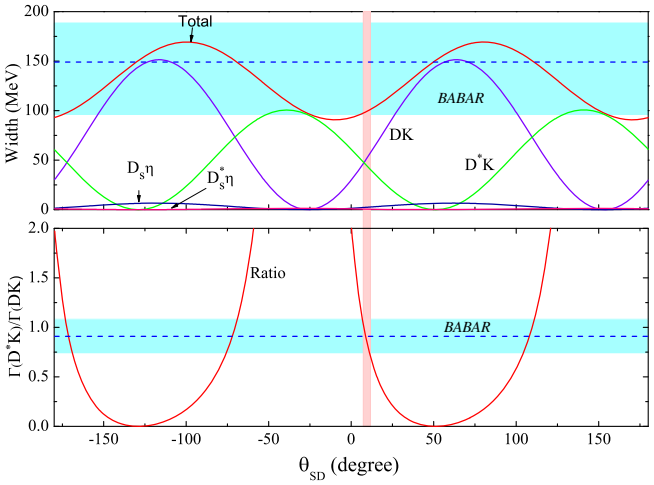

FIG. 5 (color online). The θ_{SD} dependence of the calculated partial and total decay widths and ratio $\Gamma(D^*K)/\Gamma(DK)$. The vertical band corresponds to the common range of θ_{SD}, where our results can be matched with the experimental widths and ratio [28].

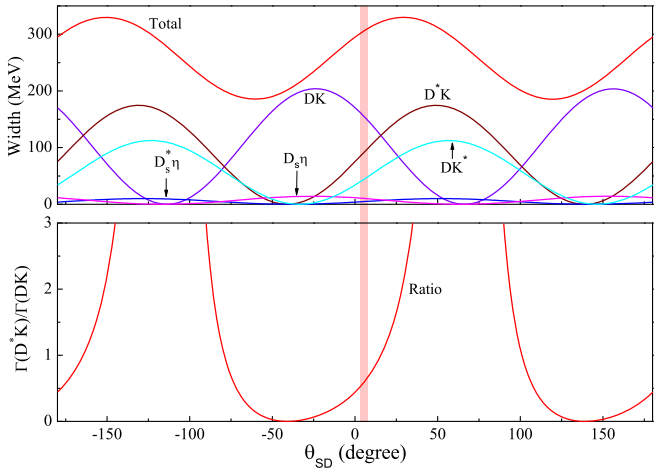

FIG. 6 (color online). The θ_{SD} dependence of the decay widths and ratio $\Gamma(D^*K)/\Gamma(DK)$ of $D^*_{s1}(2860)$. The vertical band corresponds to the common range of θ_{SD}, where our results can be matched with the experimental width and ratio of $D^*_{s1}(2700)$ [28].

that the main decay channels of $D^*_{s1}(2860)$ are DK(∼140 MeV), D^*K(∼95 MeV) and DK^*(∼50 MeV).

As an admixture of the 1^1D_2 and 1^3D_2 states, the states $1D(2^-)$ and $1D'(2^-)$ in the charmed-strange meson family satisfy the following relation:

$$\begin{pmatrix} |1D(2^-)\rangle \\ |1D'(2^-)\rangle \end{pmatrix} = \begin{pmatrix} \cos\theta_{1D} & \sin\theta_{1D} \\ -\sin\theta_{1D} & \cos\theta_{1D} \end{pmatrix} \begin{pmatrix} |1^1D_2\rangle \\ |1^3D_2\rangle \end{pmatrix}, \tag{41}$$

where θ_{1D} is a mixing angle. In the heavy quark limit, we can fix the mixing angle $\theta_{1D} = -50.8° = -\arcsin(\sqrt{3/5})$ [45,86,93]. Adopting the theoretical prediction of the masses of $D_s(1D(2^-))$ and $D_s(1D'(2^-))$ as input, we list their allowed decay channels in Table V. The θ_{1D} dependence of the partial and total decay widths of $D_s(1D(2^-))$ and $D_s(1D'(2^-))$ is given in Fig. 7. When taking the limit

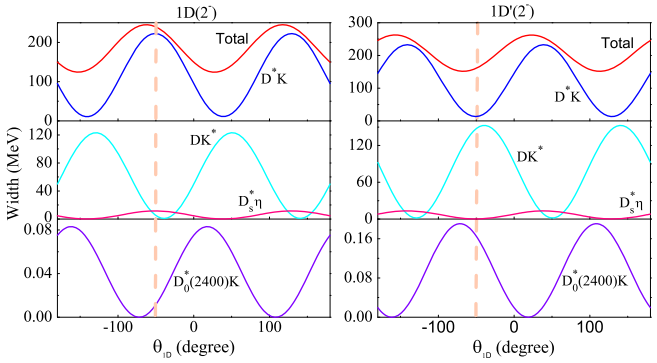

FIG. 7 (color online). The θ_{1D} dependence of the partial decay widths and the total decay width of $D_s(1D(2^-))$ (left panel) and $D_s(1D'(2^-))$ (right panel). The vertical dashed lines correspond to the mixing angle $\theta_{1D} = -50.8°$

value $\theta_{1D} = -50.8°$ [45,86,93], we conclude that the main decay modes of $D_s(1D(2^-))$ and $D_s(1D'(2^-))$ are D^*K and DK^*. In the heavy quark limit, $D_s(1D(2^-))$ couples with D^*K via a P wave, while it couples with DK^* only via an F wave due to the conservation of a light degree of freedom. As for $D_s(1D'(2^-))$, the situation is the opposite of $D_s(1D(2^-))$: $D_s(1D'(2^-))$ strongly couples with DK^* via a P wave. Our present calculations are consistent with the conclusion of the heavy quark limit [101,102], and the results are model independent in the heavy quark limit. In addition, the total decay widths of $D_s(1D(2^-))$ and $D_s(1D'(2^-))$ can reach up to 240 and 147 MeV, respectively. The above study also shows that the D^*K and DK^* modes are the key channels when distinguishing the $D_s(1D(2^-))$ and $D_s(1D'(2^-))$ states.

Besides $D^*_{s1}(2860)$, the LHCb Collaboration also observed $D^*_{s3}(2860)$. In this work, we test to see whether $D^*_{s3}(2860)$ can be a good candidate of $D_s(1^3D_3)$. The partial and total decay widths of $D^*_{s3}(2860)$ as $D_s(1^3D_3)$ are listed in Table V, in which we find that our calculated total width is about one-fourth of the experimental data [30,31]. The main decay modes of $D_s(1^3D_3)$ are DK and D^*K, where the ratio

$$\frac{\mathcal{B}(D_s(1^3D_3) \to D^{*0}K)}{\mathcal{B}(D_s(1^3D_3) \to D^0K)} = 0.802 \tag{42}$$

is obtained. We suggest doing a more precise measurement of the resonance parameters and the ratio $\mathcal{B}(D^{*0}K)/\mathcal{B}(D^0K)$ of $D^*_{s3}(2860)$, which will finally lead to a definite conclusion as to whether $D^*_{s3}(2860)$ is a $D_s(1^3D_3)$ state.

3. 2P states

There are four $2P$ states. Among these, $D_s(2^3P_0)$ and $D_s(2^3P_2)$ are still missing from experiments, while there exist possible candidates for $D_s(2P(1^+))$ and $D_s(2P'(1^+))$.

The partial and total decay widths of $D_s(2^3P_0)$ are shown in Table V, where the mass of $D_s(2^3P_0)$ is fixed as 2960 MeV (see Table II). The total decay width of $D_s(2^3P_0)$ is 166.15 MeV and there exist three main decay modes, DK, D^*K^*, and $D_1(2420)K$ (see Table V).

As for the $D_s(2^3P_2)$ state with the predicted mass 3004 MeV, the main decay modes are D^*K^*, D^*K, and $D_1(2430)K$, with the total decay width 86.25 MeV. The ratio is predicted as $\mathcal{B}(D_s(2^3P_2) \to D^*K)/\mathcal{B}(D_s(2^3P_2) \to DK^*) = 0.39$.

We notice that there is an evidence of the structure around 2960 MeV in the $\bar{D}^0K^-$ invariant mass spectrum given by LHCb [30,31] except for the observed $D^*_{s1}(2860)$ and $D^*_{s3}(2860)$. If this evidence will be confirmed by future experiments, this structure around 2960 MeV must be either $D_s(2^3P_0)$ or $D_s(2^3P_2)$ since there are no other candidates for natural states from 2800 to 3100 MeV, as shown in Fig. 2. According to the calculated decay behaviors of $D_s(2^3P_0)$ and $D_s(2^3P_2)$, we can exclude the possibility of the $D_s(2^3P_2)$ assignment to this structure since the decay width of $D_s(2^3P_2) \to DK$ is quite small.

In the following, we discuss the possibilities of the observed $D^*_{sJ}(3040)$ as $D_s(2P(1^+))$ or $D_s(2P'(1^+))$, where $D_s(2P(1^+))$ or $D_s(2P'(1^+))$ satisfy

$$\begin{pmatrix} |2P(1^+)\rangle \\ |2P'(1^+)\rangle \end{pmatrix} = \begin{pmatrix} \cos\theta_{2P} & \sin\theta_{2P} \\ -\sin\theta_{2P} & \cos\theta_{2P} \end{pmatrix} \begin{pmatrix} |2^1P_1\rangle \\ |2^3P_1\rangle \end{pmatrix}, \tag{43}$$

with a mixing angle θ_{2P}. If taking $\theta_{2P} = \theta_{1P} = -54.7°$ [45,93] to estimate the decay behaviors of $D_s(2P(1^+))$ or $D_s(2P'(1^+))$, we obtain the numerical results listed in Table V.

If assigning $D^*_{sJ}(3040)$ to $D_s(2P(1^+))$, the calculated total decay width is 285.83 MeV, which is consistent with the experimental width [28]. The main decay modes are D^*K, DK^*, D^*K^*, and $D^*_2(2460)K$, which can explain why $D^*_{sJ}(3040)$ was first observed by experiment in the D^*K channel [28]. Additionally, we predict the ratio

$$\frac{\mathcal{B}(D_s(2P(1^+)) \to D^*K)}{\mathcal{B}(D_s(2P(1^+)) \to DK^*)} = 1.59, \tag{44}$$

which can be tested by future experiments. The above study shows that $D^*_{sJ}(3040)$ is a good candidate for $D_s(2P(1^+))$, which is the first radial excitation of $D_{s1}(2460)$.

We need to discuss another possible assignment of $D^*_{sJ}(3040)$ to $D(2P'(1^+))$ if considering study of only the mass spectrum shown in Fig. 2 because the mass of $D^*_{sJ}(3040)$ is very close to the predicted mass of $D_s(2P'(1^+))$. Moreover, the total decay width of $D_s(2P'(1^+))$ is 131.28 MeV, which is comparable to the lower limit of experimental width of $D^*_{sJ}(3040)$ [28]. The predicted ratio is, however,

$$\frac{\mathcal{B}(D_s(2P'(1^+)) \to D^*K)}{\mathcal{B}(D_s(2P'(1^+)) \to DK^*)} = 3.19, \tag{45}$$

which is quite different from that given in Eq. (44). Thus, we suggest to carry out the measurement of the ratio $\mathcal{B}(D^*_{sJ}(3040) \to D^*K)/\mathcal{B}(D^*_{sJ}(3040) \to DK^*)$, which will be helpful to finally identify the inner structure of $D^*_{sJ}(3040)$.

4. 3S states

In this subsection, we predict the decay behaviors of two $3S$ states in the charmed-strange meson family, which are still missing from experiments. As shown in Table V, the partial and total decay widths of $D_s(3^1S_0)$ and $D_s(3^3S_1)$ are calculated.

As for $D_s(3^1S_0)$, the total decay width is about 111.98 MeV and the main decay channels are D^*K, D^*K^*, and $D_0^*(2400)K$. As for $D_s(3^3S_1)$, the total decay width is 115.35 MeV and the main decay channels are DK, D^*K, DK^*, and $D_1(2430)K$. This information is valuable for experimental search for these two missing $D_s(3^1S_0)$ and $D_s(3^3S_1)$ mesons.

As the unnatural state, the predicted mass (3092 MeV) of $D_s(3^1S_0)$ is very close to the mass of $D_{sJ}^*(3040)$ reported by the *BABAR* Collaboration [28]. Thus, we again check to see whether $D_{sJ}^*(3040)$ is explained by $D_s(3^1S_0)$. Since $D_{sJ}^*(3040)$ was observed in the D^*K channel, which is one of the main decay channels of $D_s(3^1S_0)$, this fact cannot exclude the possibility. However, the obtained total decay width of $D_s(3^1S_0)$ is a little bit smaller than the lower limit of the experimental width of $D_{sJ}^*(3040)$. Although the predicted $D_s(3^1S_0)$ cannot fit all of the experimental features of $D_{sJ}^*(3040)$, there exists a small possibility of $D_{sJ}^*(3040)$ as $D_s(3^1S_0)$, if considering the large experimental error of $D_{sJ}^*(3040)$. Thus, a crucial task in future experiments is the precise measurement of the resonance parameters of $D_{sJ}^*(3040)$, which can help us to come to a definite conclusion about the properties of $D_{sJ}^*(3040)$.

5. 2*D* states

There are four $2D$ states, all of which are absent from experiments. In Table VI, we predict their decay properties. As for the $D_s(2^3D_1)$ state, the predicted mass by the modified GI model is 3244 MeV and the total width obtained in the QPC model is 165.20 MeV. Its main decay channels are DK, D^*K, and $D_1(2420)K$, and the typical decay ratio is given by

$$\frac{\mathcal{B}(D_s(2^3D_1)) \to D^*K)}{\mathcal{B}(D_s(2^3D_1)) \to DK)} = 0.31. \tag{46}$$

TABLE VI. Decay behaviors of four $2D$ charmed-strange mesons (in units of MeV).

Channels	D_s (2^3D_1)	D_s $(2D(2^-))$	D_s $(2D'(2^-))$	D_s (2^3D_3)
DK	65.02	⋯	⋯	5.25
$D_s\eta$	4.13	⋯	⋯	0.23
$D_s\eta'$	0.87	⋯	⋯	0.02
D^*K	20.32	76.78	0.03	0.96
$D_s^*\eta$	0.93	4.12	0.006	0.04
$D_s^*\eta'$	0.04	0.29	0.002	3.0×10^{-7}
DK^*	5.03	4.73	30.67	0.69
$D_s\phi$	0.06	0.12	0.04	0.04
D^*K^*	3.2×10^{-4}	1.31	3.11	19.64
$D_s^*\phi$	0.37	0.42	0.47	0.36
$D_0^*(2400)K$	⋯	6.82	8.00	⋯
$D_{s0}^*(2317)\eta$	⋯	0.36	0.37	⋯
$D_0^*(2400)K^*$	0.54	0.16	0.53	0.63
$D_1(2430)K$	14.25	8.14	5.64	11.50
$D_1(2420)K$	39.90	2.80	1.71	1.26
$D_{s1}(2460)\eta$	0.59	0.32	0.24	0.43
$D_{s1}(2536)\eta$	0.19	0.07	0.06	0.007
$D_2^*(2460)K$	12.77	34.22	1.46	3.74
$D_{s2}^*(2573)\eta$	0.19	0.83	0.06	0.05
Total	165.20	141.49	52.40	44.85

As an admixture of the 2^1D_2 and 2^3D_2 states, $D_s(2D(2^-))$ and $D_s(2D'(2^-))$ satisfy the following relation:

$$\begin{pmatrix} |2D(2^-)\rangle \\ |2D'(2^-)\rangle \end{pmatrix} = \begin{pmatrix} \cos\theta_{2D} & \sin\theta_{2D} \\ -\sin\theta_{2D} & \cos\theta_{2D} \end{pmatrix} \begin{pmatrix} |2^1D_2\rangle \\ |2^3D_2\rangle \end{pmatrix}, \tag{47}$$

where the mixing angle can be fixed as $\theta_{2D} = -50.8°$ in the heavy quark limit [45,86,93] when discussing their decay behaviors.

The $D_s(2D(2^-))$ with the predicted mass 3238 MeV has the total width 141.49 MeV and its main decay channels are D^*K and $D_{s2}^*(2460)K$, which contribute to almost 80% of the total decay width. As the partner of $D_s(2D(2^-))$, $D_s(2D'(2^-))$ has the predicted mass of 3260 MeV and is a narrow state compared with $D_s(2D(2^-))$ because the total decay width is 52.4 MeV. Its main decay mode is DK^*, with a partial decay width of 30.67 MeV. The difference of the total decay widths of $D_s(2D(2^-))$ and $D_s(2D'(2^-))$ can be understood since the decays of $D_s(2D(2^-))$ and $D_s(2D'(2^-))$ into D^*K occur via P-wave and F-wave in the heavy quark limit [86], respectively.

As for the $D_s(2^3D_3)$ with mass 3251 MeV, the total decay width is 44.85 MeV and the main decay channels are D^*K^* and $D_1(2430)K$. Here, the ratio

$$\frac{\mathcal{B}(D_s(2^3D_3)) \to D^*K)}{\mathcal{B}(D_s(2^3D_3)) \to DK)} = 0.18 \tag{48}$$

is predicted via the QPC model.

6. 1*F* states

Similar to the experimental situation of the $2D$ states in the charmed-strange meson family, four $1F$ charmed-strange mesons are still missing from experiments. Thus, in the following we predict their decay behaviors.

The mass of $D_s(1^3F_2)$ is 3159 MeV predicted by the modified GI model. The OZI-allowed two-body strong decay channels are listed in Table VII. Our calculation shows that its main decay modes are DK, D^*K, DK^*, and $D_1(2420)K$. The $D_s(1^3F_2)$ is a broad state with the total decay width 415.97 MeV, where the predicted ratio is

TABLE VII. Decay behaviors of four $1F$ charmed-strange mesons (in units of MeV).

Channels	$D_s(1^3F_2)$	$D_s(1F(3^+))$	$D_s(1F'(3^+))$	$D_s(1^3F_4)$
DK	57.82	⋯	⋯	5.30
$D_s\eta$	3.16	⋯	⋯	0.11
$D_s\eta'$	0.41	⋯	⋯	0.002
D^*K	43.12	98.10	14.86	6.88
$D_s^*\eta$	2.19	4.98	0.28	0.11
$D_s^*\eta'$	0.06	0.08	4.3×10^{-4}	5.5×10^{-5}
DK^*	41.12	9.34	102.32	4.35
$D_s\phi$	0.85	0.04	2.36	0.08
D^*K^*	16.68	51.12	66.16	130.87
$D_s^*\phi$	0.01	0.002	0.09	0.01
$D_0^*(2400)K$	⋯	0.50	3.32	⋯
$D_{s0}^*(2317)\eta$	⋯	0.02	0.16	⋯
$D_1(2430)K$	0.49	0.22	0.68	1.24
$D_1(2420)K$	220.10	1.40	2.14	0.42
$D_{s1}(2460)\eta$	0.007	0.003	0.02	0.02
$D_{s1}(2536)\eta$	5.35	6.8×10^{-4}	0.004	3.0×10^{-4}
$D_2^*(2460)K$	24.34	205.68	0.95	1.40
$D_{s2}^*(2573)\eta$	0.26	0.99	7.9×10^{-4}	6.5×10^{-5}
Total	415.97	372.48	193.34	150.79

$$\frac{\mathcal{B}(D_s(2^3F_2))\to D^*K)}{\mathcal{B}(D_s(2^3F_2))\to DK)}=0.75. \tag{49}$$

The $D_s(1F(3^+))$ and $D_s(1F'(3^+))$ satisfy

$$\begin{pmatrix}|1F(3^+)\rangle\\ |1F'(3^+)\rangle\end{pmatrix}=\begin{pmatrix}\cos\theta_{1F} & \sin\theta_{1F}\\ -\sin\theta_{1F} & \cos\theta_{1F}\end{pmatrix}\begin{pmatrix}|1^1F_3\rangle\\ |1^3F_3\rangle\end{pmatrix}, \tag{50}$$

where θ_{1F} is the mixing angle, which can be determined as $\theta_{1F}=-49.1^\circ=-\arcsin(2/\sqrt{7})$ in the heavy quark limit [45,93]. In Table VII, we collect the calculated decay widths of $D_s(1F(3^+))$ and $D_s(1F'(3^+))$, where we take 3139 and 3169 MeV as their mass inputs, respectively. The main decay channels of $D_s(1F(3^+))$ are D^*K, D^*K^*, and $D_2^*(2460)K$, and the total decay width can reach up to 372.48 MeV. Thus, $D_s(1F(3^+))$ has a very broad width. As for $D_s(1F'(3^+))$, DK^* and D^*K^* are its main decay modes and the total width of $D_s(1F'(3^+))$ is 193.34 MeV.

The $D_s(1^3F_4)$ with the mass 3143 MeV dominantly decays into D^*K^* and the total decay width of $D_s(1^3F_4)$ is 150.79 MeV. In addition, we predict the following ratios:

$$\frac{\mathcal{B}(D_s(2^3F_4))\to DK)}{\mathcal{B}(D_s(2^3F_4))\to D^*K)}=0.77 \tag{51}$$

and

$$\frac{\mathcal{B}(D_s(2^3F_4))\to DK^*)}{\mathcal{B}(D_s(2^3F_4))\to DK)}=0.82, \tag{52}$$

which can be tested in future experiments.

V. SUMMARY

In the past decade, more and more charmed-strange states have been reported in different experiments which are collected in Table I. The present status of these observed charmed-strange states has stimulated us to revisit the charmed-strange meson family and to systemically carry out the study of their mass spectra and two-body OZI-allowed strong decays.

In this work, we have adopted the modified GI model to get the mass spectra of the charmed-strange meson family, where the screening effect partly reflecting the unquenched effect is considered in our calculations. Comparing the theoretical results with the experimental data, we can roughly obtain the properties of the observed charmed-strange mesons. In addition, we have also predicted the masses of the higher radial and orbital excitations in the charmed-strange meson family. This information is important in searching for these missing higher charmed-strange mesons in future experiments. Besides the mass information, in our calculation we have obtained the numerical results of the spatial wave functions of the discussed charmed-strange mesons, which are applied to calculate their two-body OZI-allowed strong decays.

To obtain the decay behaviors of the discussed charmed-strange mesons, we have adopted the QPC model in this work, where the $1P$, $2P$, $1D$, $2S$, $2D$, $3S$, and $1F$ states in the charmed-strange meson family are involved. The study of their strong decay behaviors further tests the possible assignments to the observed states, where a phenomenological analysis is performed. As for the higher charmed-strange mesons absent from the experiment, we have predicted their partial and total decay widths, and some typical decay ratios, which is valuable for the experimental study of these states.

Since 2003, the *BABAR*, Belle, CLEOc, and LHCb experiments have made much progress on the search for charmed-strange mesons. In the next ten years, we believe that more candidates for charmed-strange mesons will be reported, with the running of the LHC experiment at 14 TeV collision energy and the forthcoming Belle II and PANDA experiments. The study presented in this work is helpful in identifying these observed charmed-strange states and carrying out a search for higher radial and orbital excitations in the charmed-strange meson family.

ACKNOWLEDGMENTS

This project is supported by the National Natural Science Foundation of China under Grants No. 11222547,

No. 11175073, No. 11375240, and No. 11035006, the Ministry of Education of China (SRFDP under Grant No. 2012021111000), and the Fok Ying Tung Education Foundation (Grant No. 131006).

Note added.—Recently, we noticed a work [103] in which the authors also studied the mass spectrum and strong decays of charmed-strange mesons and obtained results similar to those in the present work.

[1] K. A. Olive *et al.* (Particle Data Group Collaboration), Review of particle physics (RPP), Chin. Phys. C **38**, 090001 (2014).

[2] S. Godfrey and N. Isgur, Mesons in a relativized quark model with chromodynamics, Phys. Rev. D **32**, 189 (1985).

[3] B. Aubert *et al.* (*BABAR* Collaboration), Observation of a Narrow Meson Decaying to $D_s^+\pi^0$ at a Mass of 2.32 GeV/c^2, Phys. Rev. Lett. **90**, 242001 (2003).

[4] D. Besson *et al.* (CLEO Collaboration), Observation of a narrow resonance of mass 2.46 GeV/c^2 decaying to $D_s^{*+}\pi^0$ and confirmation of the $D_{sJ}^*(2317)$ state, Phys. Rev. D **68**, 032002 (2003); **75**, 119908(E) (2007).

[5] K. Abe *et al.* (Belle Collaboration), Measurements of the D_{sJ} Resonance Properties, Phys. Rev. Lett. **92**, 012002 (2004).

[6] B. Aubert *et al.* (*BABAR* Collaboration), Study of the $D_{sJ}^*(2317)^+$ and $D_{sJ}(2460)^+$ mesons in inclusive $c\bar{c}$ production near $\sqrt{s} = 10.6$ GeV, Phys. Rev. D **74**, 032007 (2006).

[7] B. Aubert *et al.* (*BABAR* Collaboration), Observation of a narrow meson decaying to $D_s^+\pi^0\gamma$ at a mass of 2.458 GeV/c^2, Phys. Rev. D **69**, 031101 (2004).

[8] J. L. Goity and W. Roberts, Relativistic chiral quark model for pseudoscalar emission from heavy mesons, Phys. Rev. D **60**, 034001 (1999).

[9] M. Di Pierro and E. Eichten, Excited heavy-light systems and hadronic transitions, Phys. Rev. D **64**, 114004 (2001).

[10] W. A. Bardeen, E. J. Eichten, and C. T. Hill, Chiral multiplets of heavy-light mesons, Phys. Rev. D **68**, 054024 (2003).

[11] T. Matsuki and T. Morii, Spectroscopy of heavy mesons expanded in $1/m_Q$, Phys. Rev. D **56**, 5646 (1997).

[12] T. Matsuki, T. Morii, and K. Sudoh, New heavy-light mesons $Q\bar{q}$, Prog. Theor. Phys. **117**, 1077 (2007).

[13] T. Matsuki, T. Morii, and K. Sudoh, Radial excitations of heavy mesons, Eur. Phys. J. A **31**, 701 (2007).

[14] T. Matsuki and K. Seo, Chiral particle decay of heavy-light mesons in a relativistic potential model, Phys. Rev. D **85**, 014036 (2012).

[15] D. Ebert, V. O. Galkin, and R. N. Faustov, Mass spectrum of orbitally and radially excited heavy-light mesons in the relativistic quark model, Phys. Rev. D **57**, 5663 (1998); **59**, 019902(E) (1998).

[16] L. Micu, Decay rates of meson resonances in a quark model, Nucl. Phys. **B10**, 521 (1969).

[17] A. Le Yaouanc, L. Oliver, O. Pene, and J. C. Raynal, Naive quark pair creation model of strong interaction vertices, Phys. Rev. D **8**, 2223 (1973); Naive quark-pair—creation model and baryon decays, Phys. Rev. D **9**, 1415 (1974); Resonant partial-wave amplitudes in $\pi N \to \pi\pi N$ according to the naive quark-pair-creation model, Phys. Rev. D **11**, 1272 (1975); Why is $\psi(4.414)$ so narrow?, Phys. Lett. **72B**, 57 (1977); Strong decays of ψdblac; (4.028) as a radial excitation of charmonium, Phys. Lett. **71B**, 397 (1977).

[18] A. Le Yaouanc, L. Oliver, O. Pene, and J. C. Raynal, *Hadron Transitions in the Quark Model* (Gordon and Breach, New York, 1988).

[19] E. van Beveren, C. Dullemond, and G. Rupp, Spectrum and strong decays of charmonium, Phys. Rev. D **21**, 772 (1980); **22**, 787(E) (1980).

[20] E. van Beveren, G. Rupp, T. A. Rijken, and C. Dullemond, Radial spectra and hadronic decay widths of light and heavy mesons, Phys. Rev. D **27**, 1527 (1983).

[21] R. Bonnaz, B. Silvestre-Brac, and C. Gignoux, Radiative transitions in mesons in a nonrelativistic quark model, Eur. Phys. J. A **13**, 363 (2002).

[22] W. Roberts and B. Silvestre-Brac, General method of calculation of any hadronic decay in the $^3P_0$ model, Few-Body Syst. **11**, 171 (1992).

[23] A. E. Asratian, A. V. Fedotov, P. A. Gorichev, S. P. Kruchinin, M. A. Kubantsev, I. V. Makhlyueva, V. I. Chekelian, V. V. Ammosov *et al.*, Studying (anti-charm strange) spectroscopy in anti-neutrino N collisions, Z. Phys. C **40**, 483 (1988).

[24] Y. Kubota *et al.* (CLEO Collaboration), Observation of a New Charmed Strange Meson, Phys. Rev. Lett. **72**, 1972 (1994).

[25] A. V. Evdokimov *et al.* (SELEX Collaboration), First Observation of a Narrow Charm-Strange Meson $D_{sJ}^+(2632) \to D_s^+\eta$ and D^0K^+, Phys. Rev. Lett. **93**, 242001 (2004).

[26] B. Aubert *et al.* (*BABAR* Collaboration), Observation of a New D_s Meson Decaying to DK at a Mass of 2.86 GeV/c^2, Phys. Rev. Lett. **97**, 222001 (2006).

[27] J. Brodzicka *et al.* (Belle Collaboration), Observation of a New D_{sJ} Meson in $B^+ \to \bar{D}^0D^0K^+$ Decays, Phys. Rev. Lett. **100**, 092001 (2008).

[28] B. Aubert *et al.* (*BABAR* Collaboration), Study of D_{sJ} decays to D^*K in inclusive e^+e^- interactions, Phys. Rev. D **80**, 092003 (2009).

[29] R. Aaij *et al.* (LHCb Collaboration), Study of D_{sJ} decays to $D^+K_S^0$ and D^0K^+ final states in pp collisions, J. High Energy Phys. 10 (2012) 151.

[30] R. Aaij *et al.* (LHCb Collaboration), Observation of Overlapping Spin-1 and Spin-3 $\bar{D}^0K^-$ Resonances at Mass 2.86 GeV/c^2, Phys. Rev. Lett. **113**, 162001 (2014).

[31] R. Aaij *et al.* (LHCb Collaboration), Dalitz plot analysis of $B_s^0 \to \bar{D}^0 K^- \pi^+$ decays, Phys. Rev. D **90**, 072003 (2014).

[32] B. Aubert *et al.* (*BABAR* Collaboration), Search for the $D_{sJ}^*(2632)^+$ at *BABAR*, arXiv:hep-ex/0408087.

[33] H. Albrecht *et al.* (ARGUS Collaboration), Observation of a new charmed-strange meson, Phys. Lett. B **230**, 162 (1989).

[34] J. P. Alexander *et al.* (CLEO Collaboration), Production and decay of the $D_{s1}^+(2536)$, Phys. Lett. B **303**, 377 (1993).

[35] P. Avery *et al.* (CLEO Collaboration), *P* wave charmed mesons in e^+e^- annihilation, Phys. Rev. D **41**, 774 (1990).

[36] A. E. Asratian *et al.* (Big Bubble Chamber Neutrino Collaboration), Observation of $D_s^{**}(2536)$ meson production by neutrinos in BEBC, Z. Phys. C **61**, 563 (1994).

[37] P. L. Frabetti *et al.* (E687 Collaboration), Measurement of the Masses and Widths of $L = 1$ Charm Mesons, Phys. Rev. Lett. **72**, 324 (1994).

[38] A. Heister *et al.* (ALEPH Collaboration), Production of D_s^{**} mesons in hadronic *Z* decays, Phys. Lett. B **526**, 34 (2002).

[39] B. Aubert *et al.* (*BABAR* Collaboration), Study of resonances in exclusive *B* decays to $\bar{D}^{(*)} D^{(*)} K$, Phys. Rev. D **77**, 011102 (2008).

[40] V. M. Abazov *et al.* (D0 Collaboration), Measurement of the B_s^0 Semileptonic Branching Ratio to an Orbitally Excited D_s State, $\mathrm{Br}(B_s^0 \to D_{s1}^-(2536)\mu^+\nu X)$, Phys. Rev. Lett. **102**, 051801 (2009).

[41] S. Chekanov *et al.* (ZEUS Collaboration), Production of excited charm and charm-strange mesons at HERA, Eur. Phys. J. C **60**, 25 (2009).

[42] J. P. Lees *et al.* (*BABAR* Collaboration), Measurement of the mass and width of the $D_{s1}(2536)^+$ meson, Phys. Rev. D **83**, 072003 (2011).

[43] T. Aushev *et al.* (Belle Collaboration), Study of the decays $B \to D_{s1}(2536)^+ \bar{D}^{(*)}$, Phys. Rev. D **83**, 051102 (2011).

[44] V. Balagura *et al.* (Belle Collaboration), Observation of $D_{s1}(2536)^+ \to D^+ \pi^- K^+$ and angular decomposition of $D_{s1}(2536)^+ \to D^{*+} K_S^0$, Phys. Rev. D **77**, 032001 (2008).

[45] S. Godfrey and R. Kokoski, Properties of *p* wave mesons with one heavy quark, Phys. Rev. D **43**, 1679 (1991).

[46] R. Aaij *et al.* (LHCb Collaboration), First observation of $\bar{B}_s^0 \to D_{s2}^{*+} X \mu^- \bar{\nu}$ decays, Phys. Lett. B **698**, 14 (2011).

[47] H. Albrecht *et al.* (ARGUS Collaboration), Measurement of the decay $D_{s2}^{*+} \to D^0 K^+$, Z. Phys. C **69**, 405 (1996).

[48] T. Barnes, F. E. Close, and H. J. Lipkin, Implications of a *DK* molecule at 2.32 GeV, Phys. Rev. D **68**, 054006 (2003).

[49] H. Y. Cheng and W. S. Hou, *B* decays as spectroscope for charmed four quark states, Phys. Lett. B **566**, 193 (2003).

[50] Y. Q. Chen and X. Q. Li, Comprehensive Four-Quark Interpretation of $D_s(2317)$, $D_s(2457)$, and $D_s(2632)$, Phys. Rev. Lett. **93**, 232001 (2004).

[51] E. van Beveren and G. Rupp, Observed $D_s(2317)$ and Tentative *D* (2100–2300) as the Charmed Cousins of the Light Scalar Nonet, Phys. Rev. Lett. **91**, 012003 (2003).

[52] Y. B. Dai, X. Q. Li, S. L. Zhu, and Y. B. Zuo, Contribution of *DK* continuum in the QCD sum rule for $D_{sJ}(2317)$, Eur. Phys. J. C **55**, 249 (2008).

[53] Y. R. Liu, X. Liu, and S. L. Zhu, Light pseudoscalar meson and heavy meson scattering lengths, Phys. Rev. D **79**, 094026 (2009).

[54] B. Zhang, X. Liu, W. Z. Deng, and S. L. Zhu, $D_{sJ}(2860)$ and $D_{sJ}(2715)$, Eur. Phys. J. C **50**, 617 (2007).

[55] P. Colangelo, F. De Fazio, S. Nicotri, and M. Rizzi, Identifying $D_{sJ}(2700)$ through its decay modes, Phys. Rev. D **77**, 014012 (2008).

[56] G. L. Wang, J. M. Zhang, and Z. H. Wang, The decays of $B+ \to \bar{D}0^+ D_{sJ}^+(2S)$ and $B+ \to \bar{D}0^+ D_{sJ}^+(1D)$, Phys. Lett. B **681**, 326 (2009).

[57] F. E. Close, C. E. Thomas, O. Lakhina, and E. S. Swanson, Canonical interpretation of the $D_{sJ}(2860)$ and $D_{sJ}(2690)$, Phys. Lett. B **647**, 159 (2007).

[58] D.-M. Li and B. Ma, Implication of *BABAR*'s new data on the $D_{s1}(2710)$ and $D_{sJ}(2860)$, Phys. Rev. D **81**, 014021 (2010).

[59] X.-H. Zhong and Q. Zhao, Strong decays of newly observed D_{sJ} states in a constituent quark model with effective Lagrangians, Phys. Rev. D **81**, 014031 (2010).

[60] D. M. Li, B. Ma, and Y. H. Liu, Understanding masses of $c\bar{s}$ states in Regge phenomenology, Eur. Phys. J. C **51**, 359 (2007).

[61] P. C. Vinodkumar, A. K. Rai, B. Patel, and J. Pandya, Open flavour charmed mesons, Frascati Phys. Ser. **46**, 929 (2007).

[62] X.-h. Zhong and Q. Zhao, Strong decays of heavy-light mesons in a chiral quark model, Phys. Rev. D **78**, 014029 (2008).

[63] B. Chen, D.-X. Wang, and A. Zhang, Interpretation of $D_{sJ}(2632)^+$, $D_{s1}(2700)^{+-}$, $D_{sJ}^*(2860)^+$, and $D_{sJ}(3040)^+$, Phys. Rev. D **80**, 071502 (2009).

[64] E. van Beveren and G. Rupp, Comment on "Study of D_{sJ} decays to D^*K in inclusive e^+e^- interactions", Phys. Rev. D **81**, 118101 (2010).

[65] Q. T. Song, D. Y. Chen, X. Liu, and T. Matsuki, $D_{s1}^*(2860)$ and $D_{s3}^*(2860)$: Candidates for $1D$ charmed-strange mesons, Eur. Phys. J. C **75**, 30 (2015).

[66] S. Godfrey and K. Moats, $D_{sJ}^*(2860)$ mesons as excited *D*-wave $c\bar{s}$ states, Phys. Rev. D **90**, 117501 (2014).

[67] D. Zhou, E. L. Cui, H. X. Chen, L. S. Geng, X. Liu, and S. L. Zhu, *D*-wave heavy-light mesons from QCD sum rules, Phys. Rev. D **90**, 114035 (2014).

[68] Z.-G. Wang, $D_{s3}^*(2860)$ and $D_{s1}^*(2860)$ as the 1D $c\bar{s}$ states, Eur. Phys. J. C **75**, 25 (2015).

[69] Z. F. Sun and X. Liu, Newly observed $D_{sJ}(3040)$ and the radial excitations of *P*-wave charmed-strange mesons, Phys. Rev. D **80**, 074037 (2009).

[70] L. Y. Xiao and X. H. Zhong, Strong decays of higher excited heavy-light mesons in a chiral quark model, Phys. Rev. D **90**, 074029 (2014).

[71] P. Colangelo and F. De Fazio, Open charm meson spectroscopy: Where to place the latest piece of the puzzle, Phys. Rev. D **81**, 094001 (2010).

[72] J. Segovia, D. R. Entem, and F. Fernandez, Scaling of the $^3P_0$ strength in heavy meson strong decays, Phys. Lett. B **715**, 322 (2012).

[73] J. Segovia, D. R. Entem, F. Fernandez, and E. Hernandez, Constituent quark model description of charmonium phenomenology, Int. J. Mod. Phys. E **22**, 1330026 (2013).

[74] B.-Q. Li and K.-T. Chao, Higher charmonia and X, Y, Z states with screened potential, Phys. Rev. D **79**, 094004 (2009).

[75] S. K. Choi *et al.* (Belle Collaboration), Observation of a Narrow Charmoniumlike State in Exclusive $B^{+-} \to K^{+-}\pi^+\pi^- J/\psi$ Decays, Phys. Rev. Lett. **91**, 262001 (2003).

[76] E. J. Eichten, K. Lane, and C. Quigg, Charmonium levels near threshold and the narrow state $X(3872) \to \pi^+\pi^- J/\psi$, Phys. Rev. D **69**, 094019 (2004).

[77] K. D. Born, E. Laermann, N. Pirch, T. F. Walsh, and P. M. Zerwas, Hadron properties in lattice QCD with dynamical fermions, Phys. Rev. D **40**, 1653 (1989).

[78] G. Bali, H. Neff, T. Düssel, T. Lippert, and K. Schilling (SESAM Collaboration), Observation of string breaking in QCD, Phys. Rev. D **71**, 114513 (2005).

[79] A. Armoni, Beyond the quenched (or probe brane) approximation in lattice (or holographic) QCD, Phys. Rev. D **78**, 065017 (2008).

[80] F. Bigazzi, A. L. Cotrone, C. Nunez, and A. Paredes, Heavy quark potential with dynamical flavors: A first order transition, Phys. Rev. D **78**, 114012 (2008).

[81] Y. Namekawa *et al.*. (PACS-CS Collaboration), Charm quark system at the physical point of $2 + 1$ flavor lattice QCD, Phys. Rev. D **84**, 074505 (2011).

[82] B. Q. Li, C. Meng, and K. T. Chao, Coupled-channel and screening effects in charmonium spectrum, Phys. Rev. D **80**, 014012 (2009).

[83] E. H. Mezoir and P. Gonzalez, Is the Spectrum of Highly Excited Mesons Purely Coulombian?, Phys. Rev. Lett. **101**, 232001 (2008).

[84] K. T. Chao, Y. B. Ding, and D. H. Qin, Possible phenomenological indication for the string Coulomb term and the color screening effects in the quark–anti-quark potential, Commun. Theor. Phys. **18**, 321 (1992).

[85] Y. B. Ding, K. T. Chao, and D. H. Qin, Screened $Q\bar{Q}$ potential and spectrum of heavy quarkonium, Chin. Phys. Lett. **10**, 460 (1993).

[86] S. Godfrey and I. T. Jardine, Comment on the nature of the $D^*_{s1}(2710)$ and $D^*_{sJ}(2860)$ mesons, Phys. Rev. D **89**, 074023 (2014).

[87] Z.-C. Ye, X. Wang, X. Liu, and Q. Zhao, Mass spectrum and strong decays of isoscalar tensor mesons, Phys. Rev. D **86**, 054025 (2012).

[88] C. Hayne and N. Isgur, Beyond the wave function at the origin: Some momentum dependent effects in the nonrelativistic quark model, Phys. Rev. D **25**, 1944 (1982).

[89] M. Jacob and G. C. Wick, On the general theory of collisions for particles with spin, Ann. Phys. (N.Y.) **7**, 404 (1959); On the general theory of collisions for particles with spin, Ann. Phys. (N.Y.) **281**, 774 (2000).

[90] J. Lu, X. L. Chen, W. Z. Deng, and S. L. Zhu, Pionic decays of $D_{sj}(2317)$, $D_{sj}(2460)$ and $B_{sj}(5718)$, $B_{sj}(5765)$, Phys. Rev. D **73**, 054012 (2006).

[91] P. L. Cho and M. B. Wise, Comment on $D^*_s \to D_s\pi^0$ decay, Phys. Rev. D **49**, 6228 (1994).

[92] J. Gasser and H. Leutwyler, Chiral perturbation theory: Expansions in the mass of the strange quark, Nucl. Phys. **B250**, 465 (1985).

[93] T. Matsuki, T. Morii, and K. Seo, Mixing angle between $^3P_1$ and $^1P_1$ in HQET, Prog. Theor. Phys. **124**, 285 (2010). Sometimes, people adopt different expressions for the mixing states between $^1L_1$ and $^3L_1$, whose detail is given in this paper. A correction to this paper is in order, as

$$\begin{pmatrix} \cos\theta & \sin\theta \\ -\sin\theta & \cos\theta \end{pmatrix} \begin{pmatrix} |^1P_1\rangle \\ |^3P_1\rangle \end{pmatrix} = \begin{pmatrix} \cos(\theta - 90°) & \sin(\theta - 90°) \\ -\sin(\theta - 90°) & \cos(\theta - 90°) \end{pmatrix} \begin{pmatrix} |^3P_1\rangle \\ -|^1P_1\rangle \end{pmatrix}.$$

Therefore, two definitions for the mixing angles given in Refs. [45,93] are equivalent; i.e., $\theta = 35.3°$ is equivalent to $\theta - 90° = -54.7°$. The lhs is in Ref. [93] and the rhs is given in Ref. [45].

[94] T. Barnes, S. Godfrey, and E. S. Swanson, Higher charmonia, Phys. Rev. D **72**, 054026 (2005).

[95] Fayyazuddin and Riazuddin, Some comments on narrow resonances $D^*_{s1}(2.46\ \mathrm{GeV}/c^2)$ and $D_{s0}(2.317\ \mathrm{GeV}/c^2)$, Phys. Rev. D **69**, 114008 (2004).

[96] S. Godfrey, Testing the nature of the $D^*_{sJ}(2317)^+$ and $D_{sJ}(2463)^+$ states using radiative transitions, Phys. Lett. B **568**, 254 (2003).

[97] W. Wei, P. Z. Huang, and S. L. Zhu, Strong decays of $D_{sJ}(2317)$ and $D_{sJ}(2460)$, Phys. Rev. D **73**, 034004 (2006).

[98] P. Colangelo and F. De Fazio, Understanding $D_{sJ}(2317)$, Phys. Lett. B **570**, 180 (2003).

[99] S. Ishida, M. Ishida, T. Komada, T. Maeda, M. Oda, K. Yamada, and I. Yamauchi, The $D_s(2317)$ and $D_s(2463)$ mesons as scalar and axial vector chiralons in the covariant level classification scheme, AIP Conf. Proc. **717**, 716 (2004).

[100] J. L. Rosner, P wave mesons with one heavy quark, Comments Nucl. Part. Phys. **16**, 109 (1986).

[101] F. E. Close and E. S. Swanson, Dynamics and decay of heavy-light hadrons, Phys. Rev. D **72**, 094004 (2005).

[102] T. J. Burns, Angular momentum coefficients for meson strong decay and unquenched quark models, Phys. Rev. D **90**, 034009 (2014).

[103] J. Segovia, D. R. Entem, and F. Fernandez, Charmed-strange meson spectrum: Old and new problems, arXiv: 1502.03827.